NASA TM X-175

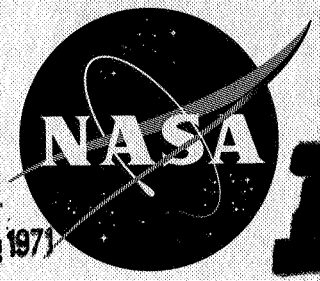

TECHNICAL MEMORANDUM

X-175

AERODYNAMIC CHARACTERISTICS AT MACH NUMBERS FROM 2.29 TO 4.65 OF 80° SWEPT ARROW WINGS WITH AND WITHOUT CAMBER AND TWIST

By Dennis F. Hasson and Norman Wong

Langley Research Center
Langley Field, Va.

NATIONAL AERONAUTICS AND SPACE ADMINISTRATION
WASHINGTON
January 1960

NATIONAL AERONAUTICS AND SPACE ADMINISTRATION

TECHNICAL MEMORANDUM X-175

AERODYNAMIC CHARACTERISTICS AT MACH NUMBERS FROM 2.29 TO 4.65 OF 80° SWEPT ARROW WINGS WITH AND WITHOUT CAMBER AND TWIST*

By Dennis F. Hasson and Norman Wong

SUMMARY

An investigation has been conducted to determine the lift, drag, and pitching-moment characteristics of a cambered and twisted arrow wing and an uncambered and untwisted arrow wing. The cambered and twisted wing was designed to give a high value of maximum lift-drag ratio at a lift coefficient of 0.08 at a Mach number of 3.0. Each wing had a leading-edge sweep of 80°, an aspect ratio of 1.085, a taper ratio of 0, and a notch ratio of 0.65. A 2.5-percent streamwise thickness distribution was centered on the mean camber surface of both wings.

Tests were conducted at Mach numbers of 2.29, 2.98, 3.96, and 4.65 with transition fixed. The Reynolds number based on the mean aerodynamic chord for most of the tests was 5.0×10^6. Additional tests at a Mach number of 2.98 were made at Reynolds numbers of 12.7×10^6 and 16.1×10^6 on the cambered and twisted wing and 12.7×10^6 and 14.9×10^6 on the wing without camber and twist.

The experimental maximum lift-drag ratio at a Mach number of 2.98 and a Reynolds number of 5.0×10^6 for the cambered and twisted wing was 7.50 and, thus, was below the theoretical estimate of 9.1. At a Mach number of 2.98 the cambered and twisted wing showed a 0.4 increase in lift-drag ratio over the wing without camber and twist. This increment in maximum lift-drag ratio due to camber and twist decreased with increasing Mach number up to a Mach number of approximately 3.68; from M = 3.68 to M = 4.65 the wing without camber and twist had higher values of lift-drag ratio than did the wing with camber and twist. The highest value of maximum lift-drag ratio at the design Mach number was 8.0 at a Reynolds number of 16.1×10^6.

---

* Title, Unclassified.

With the moment reference centers at 0.474 of the mean aerodynamic chord, both wings were longitudinally stable at lift coefficients below the design lift coefficient at all test Mach numbers except at a Mach number of 4.65 where the cambered and twisted wing became neutrally stable. At lift coefficients near or above the design lift coefficient, a nonlinear change in pitching-moment coefficients developed that resulted in instability tendencies for both wings.

INTRODUCTION

Current interest in the development of airplane configurations having long-range capabilities at supersonic speeds has resulted in extensive investigation of arrangements designed to produce high values of maximum lift-drag ratio. One approach to this problem has been the utilization of camber and twist on wings with subsonic leading edges in order to obtain optimum wing load distributions because of the substantial gains indicated by linear theory. A number of experimental investigations have been conducted to evaluate this approach (for example, refs. 1, 2, and 3).

The wing for the current tests was designed by the Theoretical Mechanics Division of the Langley Research Center as part of a program to investigate the drag-due-to-lift characteristics of cambered arrow wings with subsonic leading edges. In a previous investigation a cambered and twisted wing designed for a Mach number of 3.0 and incorporating 75° of leading-edge sweep was expected to give minimum induced drag at a lift coefficient of 0.1. The results of that investigation (ref. 1) indicated that high negative pressures on the upper surface of the wing induced supercritical velocity components normal to the leading edge. This characteristic of arrow wing camber surfaces designed for minimum drag led to flow separation and shock formation, and the wing did not exhibit the advantages predicted by linear theory. The design criterion used herein is to employ camber and twist of such a nature as to give a minimum theoretical induced drag consistent with the avoidance of conditions that lead to supercritical flow. To obtain the Mach number components normal to the leading edge of slightly less than 1.0, the camber surface, the leading-edge sweep angle of 80°, and the design lift coefficient of 0.08 were selected for the current wing at the design Mach number of 3.0. A 2.5-percent streamwise circular-arc thickness distribution was used since it was felt that the pressure characteristics of this section would not adversely affect the pressure distribution over the wing. An uncambered and untwisted arrow wing of the same plan form and thickness was provided in order to compare the two wings.

Both wings were tested in the Langley Unitary Plan wind tunnel at Mach numbers of 2.29, 2.98, 3.96, and 4.65. The Reynolds number based on the mean aerodynamic chord for most of the tests was 5.0 x 10^6.

Additional tests at a Mach number of 2.98 were made at Reynolds numbers of 12.7×10^6 and 16.1×10^6 on the wing with camber and twist and 12.7×10^6 and 14.9×10^6 on the wing without camber and twist.

SYMBOLS

The force- and moment-coefficient data are presented about the wind axes system. The reference centers and reference planes are shown in figure 1.

$\bar{c}$	wing mean aerodynamic chord, 21.67 in.
C_D'	drag coefficient, $\frac{\text{Drag}}{qS}$
$C_{D,b}'$	base drag coefficient, $\frac{\text{Base drag}}{qS}$
C_L	lift coefficient, $\frac{\text{Lift}}{qS}$
C_m	pitching-moment coefficient, $\frac{\text{Pitching moment}}{qSl}$
C_{L_α}	lift-curve slope, per deg
l	total length of model in streamwise direction, wing apex to wing tip, 50.00 in.
L/D	lift-drag ratio
$\frac{\partial C_D'}{\partial C_L^2}$	drag-due-to-lift factor, $\frac{C_D' - (C_{D,min}')_{\text{flat wing}}}{C_L^2 \text{ for } (L/D)_{max}}$
$\frac{\partial C_m}{\partial C_L}$	longitudinal stability parameter ($C_L \approx 0$)
M	free-stream Mach number
p	free-stream static pressure, lb/sq ft
q	free-stream dynamic pressure, $0.7pM^2$, lb/sq ft
R	Reynolds number based on mean aerodynamic chord
S	total wing area, 1.99 sq ft
x	distance parallel to wing center line, in.
Y	distance perpendicular to wing center line, in.

z ordinate, measured normal to wing reference plane (table II), in.

α angle of attack of the reference plane, deg

Subscripts:

c camber surface

l lower surface

max maximum value

min minimum value

u upper surface

MODELS AND APPARATUS

Dimensional details and photographs of the models tested are presented in figures 1 and 2. The geometric characteristics of the models are given in table I. The ordinates for the cambered and twisted wing are given in table II. No ordinates are given for the wing without camber and twist. This wing is called the flat wing hereinafter in the text. Both wings have a 2.5-percent biconvex streamwise thickness distribution.

A minimum center body was placed on each model to provide a balance housing. The center body for the flat wing (fig. 1(a)) consisted of a cone cylinder. However, the center body for the cambered and twisted wing differed somewhat from a cone cylinder as indicated in figure 1(b).

Forces and moments on the model were measured by means of a six-component internal strain-gage balance. This balance was attached, by means of a sting, to the tunnel central support system.

The tests were conducted in the high Mach number test section of the Langley Unitary Plan wind tunnel which is a variable-pressure, continuous-flow tunnel. The test section is 4 feet square and approximately 7 feet in length and is equipped with an asymmetric sliding-block-type nozzle which allows a continuous variation of Mach numbers from 2.29 to 4.65.

TESTS

The tests were conducted at the conditions indicated in the following table:

Mach number	Reynolds number (based on E)	Stagnation pressure, lb/sq in. abs	Dynamic pressure, lb/sq ft	Stagnation temperature, °F
2.29	5.0×10^6	14.6	629	150
2.98	5.0×10^6	21.0	530	150
	12.7	53.3	1,345	150
	14.9	62.5	1,578	150
	16.1	67.3	1,699	150
3.96	5.0×10^6	37.2	408	175
4.65	5.0×10^6	50.8	318	175

The dewpoint for all tests was maintained at less than -30° F. The angle-of-attack range was from -4° to 10° for the flat wing and from -12° to 4° for the cambered and twisted wing. Transition was fixed for all tests.

The transition strips consisted of bands of sand 1/32 inch wide applied at 5 percent of the local streamwise chord on the wing with a density of about 100 grains per square inch. The grain height was 0.011 inch to 0.013 inch.

In order to indicate the flow conditions on the upper surface of the cambered and twisted wing, a fluorescent oil was painted on the wing surface. A description of this technique is given in reference 4. The model was translated forward and rearward in the test section to obtain photographic coverage of the wing, and the resulting prints were assembled to form composite photographs (fig. 3).

CORRECTIONS AND ACCURACY

The maximum deviation of local Mach number in the part of the test section occupied by the model is ±0.015 from the average value given for the lower two Mach numbers and ±0.05 and 50.04 for the nominal Mach numbers of 3.96 and 4.65, respectively. The pressure gradients are sufficiently small so that no buoyancy correction is required.

The average angularity of the flow in the region of the models was evaluated by comparing the normal-force-coefficient variation of the inverted and upright tests, and the angle of attack was adjusted to

bring differences between these tests into agreement. The angles of attack have also been corrected for balance-sting deflection.

The data have been adjusted to the condition of free-stream static pressure on the base of the model center body.

Based upon balance accuracy and repeatability of data, it is estimated that the data are accurate within the following limits:

C_L	±0.002
C'_D	±0.0005
$C'_{D,b}$	±0.0005
C_m	±0.0005
α, deg	±0.1

PRESENTATION OF RESULTS

The results of this investigation are presented in the following figures:

	Figure
Variation of base drag coefficient with angle of attack for various Mach numbers at R = 5.0 x 10^6	4
Variation of base drag coefficient with angle of attack for various Reynolds numbers at M = 2.98	5
Basic aerodynamic characteristics	6
Comparison of theoretical and experimental results at M = 2.98	7
Summary of the aerodynamic characteristics	8
Comparison of the variation of $C'_{D,min}$ and $(L/D)_{max}$ with Mach number of cambered and twisted arrow wings	9
Effect of Reynolds number on basic aerodynamic characteristics at M = 2.98	10
Variation of $C'_{D,min}$ and $(L/D)_{max}$ with Reynolds number at M = 2.98	11

DISCUSSION

Performance

At a Mach number of 2.98, which corresponds closely to the design Mach number, and at a design lift coefficient of 0.08, the cambered and twisted wing produced a maximum lift-drag ratio of 7.5 compared with 7.1 for the flat wing (fig. 7). Both wings had lift-drag ratios slightly higher than the no leading-edge suction estimate of 6.8. However, the cambered and twisted wing failed by a considerable margin to achieve the theoretical level of 9.1. This result is reflected in a comparison of the drag-due-to-lift factors $\frac{\partial C_D'}{\partial C_L^2}$ (ref. 5), which were 0.340 for theory as compared with 0.838 for the experiment. It should be emphasized that the drag due to lift was computed by using the flat-wing minimum drag values as suggested in reference 5. It is pointed out that this method of computation does not consider the shape of the drag polars. These higher experimental values of drag could result from the presence of shocks on the wing and attendant flow separation as found in a similar investigation of a 74° swept cambered and twisted arrow wing (ref. 3). The pitching-moment curves (fig. 6) show destabilizing breaks at lift coefficients near those for maximum lift-drag ratio; this gives a strong indication that a change in the expected loading is taking place on the wings. The flow photographs (fig. 3) which were made at lift coefficients below the design lift coefficient of the wing showed no shocks and only minor flow separation at the trailing edge on the upper surface of the wing.

The cambered and twisted wing had higher values of maximum lift-drag ratio than did the flat wing up to a Mach number of approximately 3.65, where the flat wing became more efficient (fig. 8).

In general, both the wings showed the usual decrease in maximum lift-drag ratio with increasing Mach number. The values went from 7.8 and 7.1 at M = 2.29 to 6.5 and 7.05 at M = 4.65 for the cambered wing and the flat wing, respectively. The values of $\frac{\partial C_D'}{\partial C_L^2}$ for both wings (fig. 8) were lower than the values of $1/C_{L_\alpha}$ ($1/C_{L_\alpha}$ corresponds to the case of no leading-edge suction) up to a Mach number of approximately 4.2, where $\frac{\partial C_D'}{\partial C_L^2}$ became greater than $1/C_{L_\alpha}$. Thus, both wings realized some so-called leading-edge suction below a Mach number of 4.2.

A comparison of the cambered and twisted wings of the present investigation and of reference 1 is given in figure 9. The 80° wing at the design Mach number of 3.0 has an increment of about 1.0 in lift-drag ratio over the wing investigated in reference 1, and this favorable increment is probably due to the lower value of minimum drag of the 80° wing. These results show that, although the design lift coefficient was decreased and the leading-edge sweep was increased for the present wing, apparently it is rather difficult to attain the linear-theory prediction for cambered and twisted wings of high maximum lift-drag ratios at this time.

The data at higher Reynolds numbers at a Mach number of 2.98 for the flat and cambered wings (fig. 10) do not show any unusual results. In figure 11, the maximum lift-drag ratio for the cambered and twisted wing increases about 0.5 to a value of 8.0 in a Reynolds number range from 5.0×10^6 to 16.1×10^6, whereas that for the flat wing increases about 0.6 to a value of 7.7 in a Reynolds number range from 5.0×10^6 to 14.9×10^6. Since the shape of the drag polars is almost the same throughout the Reynolds number range for both wings, the drag due to lift does not change appreciably and the increments in lift-drag ratio due to increasing Reynolds number are directly attributed to the lower values of minimum drag at the higher Reynolds numbers.

L 5 6 0

Longitudinal Stability

Examination of the pitching-moment curves (fig. 6) shows that the cambered and twisted wing develops positive pitching moments at zero lift coefficient throughout the Mach number range of the tests. This is a favorable effect, since for some static margin $\left(\text{e.g.}, -\frac{\partial C_m}{\partial C_L}\right)$ the wing could be made to trim exactly at the lift coefficient for $(L/D)_{max}$. Thus there would be no loss in $(L/D)_{max}$ due to trimming the wing.

With the moment reference centers at $0.474\bar{c}$, both wings had static longitudinal stability $\left(-\frac{\partial C_m}{\partial C_L}\right)$ at all Mach numbers of the tests except at a Mach number of 4.65 where the static longitudinal stability $\left(\frac{\partial C_m}{\partial C_L} = 0\right)$ became neutral for the cambered and twisted wing (fig. 8). Destabilizing breaks in the pitching-moment curves occurred at low positive lift coefficients at all test Mach numbers (fig. 6). The pitching-moment curves for both wings at the higher Reynolds numbers (fig. 10) do not show any significant changes when compared with the data at a Reynolds number of 5.0×10^6.

The aerodynamic-center location varied from 0.549$\bar{c}$ to 0.474$\bar{c}$ for the cambered and twisted wing and from 0.554$\bar{c}$ to 0.516$\bar{c}$ for the flat wing between Mach numbers of 2.29 and 4.65.

SUMMARY OF RESULTS

Results of this investigation may be summarized as follows: At a Mach number of 2.98 and a Reynolds number of 5.0×10^6, the experimental maximum lift-drag ratio for the cambered and twisted wing was 7.5 as compared with the theoretically predicted value of 9.1 for the design Mach number of 3.00. The cambered and twisted wing showed a 0.4 increase in lift-drag ratio over the flat wing at a Mach number of 2.98. The value of maximum lift-drag ratio at the design Mach number increased with increasing Reynolds number and reached a value of 8.0 at a Reynolds number of 16.1×10^6.

Both wings with a moment center at 0.474$\bar{c}$ had static longitudinal stability near zero lift coefficient throughout the Mach number range, except at a Mach number of 4.65 where the cambered and twisted wing became neutrally stable.

Langley Research Center,
National Aeronautics and Space Administration,
Langley Field, Va., August 11, 1959.

[redacted]

REFERENCES

1. Hallissy, Joseph M., Jr., and Hasson, Dennis F.: Aerodynamic Characteristics at Mach Numbers 2.36 and 2.87 of an Airplane Configuration Having a Cambered Arrow Wing With a 75° Swept Leading Edge. NACA RM L58E21, 1958.

2. Katzen, Elliott D.: Idealized Wings and Wing Bodies at a Mach Number of 3. NACA TN 4361, 1958.

3. Hasson, Dennis F., Fichter, Ann B., and Wong, Norman: Aerodynamic Characteristics at Mach Numbers From 1.6 to 2.8 of 74° Swept Arrow Wings With and Without Camber and Twist. NASA TM X-8, 1959.

4. Loving, Donald L., and Katzoff, S.: The Fluorescent-Oil Film Method and Other Techniques for Boundary-Layer Flow Visualization. NASA MEMO 3-17-59L, 1959.

5. Baals, Donald D., Toll, Thomas A., and Morris, Owen G.: Airplane Configurations for Cruise at a Mach Number of 3. NACA RM L58E14a, 1958.

L 5 6 0

[redacted]

TABLE I.- GEOMETRIC CHARACTERISTICS OF THE MODELS

Bodies:	
Length, in. -	
Flat arrow wing	34.36
Cambered and twisted wing	33.86
Diameter of body on flat wing, in.	1.875
Width of body on cambered and twisted wing, in.	1.374
Base area, sq in. -	
Flat arrow wing	2.765
Cambered and twisted arrow wing	2.390
Wings:	
Area, sq ft	1.99
Span, in.	17.632
Aspect ratio	1.085
Taper ratio	0
Sweepback of leading edge, deg	80.0
Sweepback of trailing edge, deg	63.37
Total length in streamwise direction, wing apex to wing tip, in.	50.00
Mean aerodynamic chord, in.	21.67
Mean-aerodynamic-chord location, in. -	
Lateral distance from body center line	2.939
Longitudinal distance from nose	16.67
Notch ratio, $\frac{\text{Theoretical root chord, in.}}{\text{Total length of wing, in.}}$	0.65

TABLE 11.- ORDINATES FOR 80° SWEPT ARROW WING WITH CAMBER AND TWIST

[Ordinates are nondimensional; positive directions are indicated by arrows in sketch]

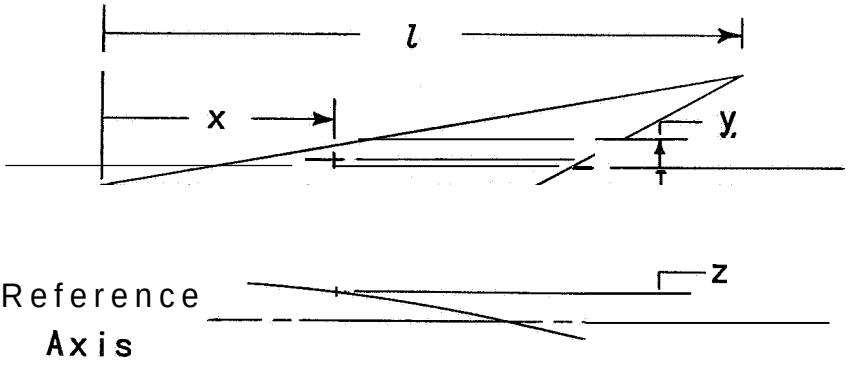

$\frac{y}{l}$	$\frac{z_c}{l}$	$\frac{z_u}{l}$	$\frac{z_l}{l}$
$\frac{x}{l}$ = 0			
0	0.0457	0.0457	0.0457
$\frac{x}{l}$ = 0.05			
0	0.04000	0.04227	0.03773
.00035	.04000	.04218	.03782
.00071	.04000	.04208	.03792
.00123	.04000	.04196	.03804
.00212	.04000	.04171	.03829
.00353	.03990	.04127	.03853
.00494	.03930	.04034	.03826
.00661	.03790	.03846	.03734
.00758	.03690	.03723	.03657
.00811	.03620	.03640	.03600
.00838	.03580	.03592	.03568
.00855	.03560	.03566	.03554
.00873	.03530	.03532	.03528
.00882	.03500	.03500	.03500

$\frac{y}{l}$	$\frac{z_c}{l}$	$\frac{z_u}{l}$	$\frac{z_l}{l}$
$\frac{X}{b}$ = 0.10			
0	0.03440	0.03861	0.03019
.00071	.03450	.03855	.03045
.00141	.03451	.03843	.03061
.00247	.03452	.03820	.03084
.00423	.03449	.03779	.03119
.00705	.03408	.03678	.03138
.00987	.03320	.03520	.03120
.01322	.03075	.03190	.02960
.01516	.02870	.02936	.02804
.01622	.02725	.02763	.02687
.01675	.02648	.02672	.02624
.01710	.02600	.02612	.02588
.01746	.02540	.02544	.02536
.01763	.02520	.02520	.02520
$\frac{x}{l}$ = 0.15			
	0.02890	0.03466	0.02314
.00106	.02900	.03459	.02341
.00212	.02908	.03446	.02368
.00370	.02908	.03420	.02396
.00635	.02900	.03365	.02435
.01058	.02850	.03229	.02471
.01481	.02723	.03012	.02434
.01984	.02385	.02250	.02215
.02275	.02098	.02195	.02001
.02433	.01912	.01968	.01856
.02513	.01815	.01850	.01780
.02566	.01725	.01745	.01703
.02618	.01653	.01659	.01647
.02645	.01610	.01610	.01610

TABLE 11.- ORDINATES FOR 80° SWEPT ARROW WING WITH CAMBER AND TWIST - Continued

$\frac{y}{l}$	$\frac{z_c}{l}$	$\frac{z_u}{l}$	$\frac{z_l}{l}$
$\frac{x}{l}$ = 0.30			
0	0.02350	0.63036	0.01664
.00141	.02355	.03028	.01682
.00282	.02360	.03015	.01705
.00494	.02355	.02978	.01732
.00846	.02345	.02930	.01770
.01411	.02320	.02798	.01842
.01975	.02170	.02539	.01801
.02645	.01755	.01978	.01532
.03033	.01445	.01575	.01315
.03244	.01250	.01326	.01174
.03350	.01140	.01187	.01093
.03421	.01075	.01103	.01047
.03491	.01000	.01010	.00990
.03527	.00952	.00952	.00952
$\frac{x}{l}$ = 0.35			
0	0.01800	0.02569	0.01031
.00176	.01804	.02556	.01052
.00353	.01810	.02544	.01076
.00617	.01815	.02521	.01109
.01058	.01815	.02468	.01162
.01763	.01760	.02318	.01202
.02469	.01585	.02025	.01145
.03306	.01250	.01523	.00977
.03791	.01020	.01178	.00862
.04056	.00860	.00953	.00767
.04188	.00780	.00839	.00721
.04276	.00705	.00739	.00671
.04364	.00640	.00650	.00630
.04408	.00600	.00600	.00600

$\frac{y}{l}$	$\frac{z_c}{l}$	$\frac{z_u}{l}$	$\frac{z_l}{l}$
$\frac{x}{l}$ = 0.30			
0	0.01300	0.02107	0.00493
.00212	.01305	.02098	.00512
.00423	.01308	.02087	.00529
.00741	.01311	.02067	.00555
.01270	.01305	.02013	.00597
.02116	.01248	.01863	.00633
.02962	.01120	.01619	.00621
.03967	.00910	.01226	.00594
.04549	.00790	.00980	.00600
.04867	.00680	.00791	.00569
.05025	.00620	.00690	.00550
.05131	.00540	.00584	.00496
.05237	.00480	.00495	.00465
.05290	.00445	.00445	.00445
$\frac{x}{l}$ = 0.35			
0	0.00725	0.01532	-0.00082
.00247	.00725	.01523	-.00073
.00494	.00725	.01513	-.00063
.00864	.00725	.01496	-.00046
.01481	.00725	.01461	-.00011
.02469	.00725	.01381	.00069
.03456	.00725	.01268	.00182
.04629	.00725	.01082	.00368
.05307	.00725	.00942	.00508
.05678	.00710	.00838	.00582
.05863	.00670	.00753	.00587
.05986	.00631	.00682	.00580
.06110	.00565	.00582	.00548
.06171	.00504	.00504	.00504

TABLE 11.- ORDINATES FOR 80° SWEPT ARROW WING WITH CAMBER AND TWIST - Continued

$\frac{y}{l}$	$\frac{z_c}{l}$	$\frac{z_u}{l}$	$\frac{z_l}{l}$
$\frac{x}{l}$ = 0.40			
)	0.00170	0.00939	-0.00599
.00282	.00160	.00926	-.00606
.00564	.00155	.00919	-.00609
.00987	.00155	.00910	-.00600
.01693	.00165	.00898	-.00568
.02821	.00245	.00917	-.00427
.03950	.00400	.00973	-.00173
.05290	.00655	.01046	.00264
.06066	.00806	.01048	.00562
.06489	.00801	.00945	.00657
.06700	.00760	.00852	.00668
.06841	.00716	.00773	.00659
.06983	.00641	.00659	.00623
.07053	.00573	.00573	.00573
$\frac{x}{l}$ = 0.45			
)	-0.00400	0.00286	-0.01086
.00317	-.00400	.00298	-.01098
.00635	-.00395	.00307	-.01097
.01111	-.00390	.00316	-.01096
.01904	-.00350	.00352	-.01052
.03174	-.00175	.00491	-.00841
.04443	.00190	.00777	-.00397
.05951	.00722	.01138	.00306
.06824	.00896	.01159	.00633
.07300	.00893	.01053	.00733
.07538	.00848	.00951	.00745
.07697	.00799	.00862	.00736
.07855	.00716	.00738	.00694
.07935	.00640	.00640	.00640

$\frac{y}{l}$	$\frac{z_c}{l}$	$\frac{z_u}{l}$	$\frac{z_l}{l}$
0	-0.00970	-0.00396	-0.01546
.00353	-.00956	-.00364	-.01548
.00705	-.00950	-.00346	-.01554
.01234	-.00920	-.00300	-.01540
.01587	-.00895	-.00266	-.01524
.02116	-.00847	-.00210	-.01484
.02821	-.00745	-.00104	-.01386
.03527	-.00530	.00105	-.01165
.04232	-.00250	.00365	-.00865
.04937	.00050	.00633	-.00533
.05731	.00421	.00947	-.00105
.06612	.00784	.01216	.00352
.07229	.00936	.01280	.00592
.07582	.00983	.01266	.00700
.07935	.00993	.01206	.00780
.08111	.00983	.01158	.00808
.08287	.00956	.01091	.00821
.08376	.00935	.01048	.00822
.08552	.00882	.00952	.00812
.08640	.00840	.00880	.00800
.08816	.00706	.00706	.00706
$\frac{x}{l}$ = 0.55			
0	-0.01530	-0.01109	-0.01951
.00388	-.01515	-.01069	-.01961
.00776	-.01500	-.01030	-.01970
.01358	-.01462	-.00961	-.01963
.01746	-.01430	-.00911	-.01949
.02328	-.01352	-.00810	-.01894
.03103	-.01180	-.00617	-.01743
.03879	-.00860	-.00284	-.01436
.04655	-.00450	.00125	-.01025
.05431	-.00015	.00543	-.a573
.06304	.00441	.00960	-.00078
.07273	.00843	.01282	.00404
.07952	.01014	.01371	.00657
.08340	.01067	.01363	.00768
.08728	.01081	.01309	.00853
.08922	.01072	.01260	.00884
.09116	.01043	.01189	.00897
.09213	.01020	.01144	.00896
.09407	.00963	.01039	.00887
.04504	.00918	.00970	.00866
.09698	.00771	.00771	.00771

TABLE II.- ORDINATES FOR 80° SWEPT *ARROW* WING WITH CAMBER AND TWIST - **Continued**

$\frac{y}{l}$	$\frac{z_c}{l}$	$\frac{z_u}{l}$	$\frac{z_l}{l}$
$\frac{x}{l}$ = 0.60			
0	-0 092150	-0.01923	-0.02377
.00423	-.02115	-.01850	-.02380
.00846	-.02065	-.01767	-.02363
.01481	-.01980	-.01636	-.02324
.01904	-091900	-.01529	-.02271
.02539	-.01770	-.01359	-.02181
.03385	**-091510**	-.01044	-.01966
.04232	-.01128	-.00640	-.01616
.05078	-.00625	-.00117	-.01133
.05925	-.00078	.00434	-.00590
.06877	.00458	.00952	-.00036
.07935	.00898	.01333	.00463
.08675	.01089	.01452	.00726
.09098	.01149	.01457	.00831
.09522	.01167	.01407	.00927
.09733	.01158	.01357	.00959
.09945	.01128	.01284	.00972
.10051	.01103	.01236	.00970
.10262	.01042	.01124	.00960
.10368	.00994	.01050	.00938
.10580	.00835	.00835	.00835
$\frac{x}{l}$ = 0.45			
0	-0.02745	-0.02745	-0.02745
.00458	-.02700	-.02655	-.02745
.00917	-.02650	-.02561	-.92739
.01605	-.02555	-.02404	-.02707
.02063	-.02470	-.02280	-.02660
.02751	-.02290	-.02044	-.02536
.03668	-.01930	-.01618	-.02242
.04585	-.01390	-.01021	-.01759
.05501	-.00759	-.00346	-.01172
.06418	-.00107	.00333	-.00547
.07450	.00469	.00917	.00021
.08596	.00950	.01366	.00534
.09398	.01160	.01519	.00801
.09857	.01229	.01539	.00919
.10315	.01251	.01498	.01004
.10544	.01243	.01451	.01035
.10774	.01211	.01375	.01047
.10888	.01186	.01325	.01047
.11117	.01121	.01209	.01033
.11232	.01069	.01129	.01009
.11461	.00898	.00898	.00898

$\frac{y}{l}$	$\frac{z_c}{l}$	$\frac{z_u}{l}$	$\frac{z_l}{l}$
$\frac{x}{l}$ = 0.70			
0.02519	-0.02825	-0.02825	-0.02825
.02962	-.02715	-.02668	-.02762
.03950	-.02240	-.02106	-.02374
.04937	-.01600	-.01385	-.01815
.05925	-.00834	-.00549	-.01119
.06912	-.00140	090200	-.00480
.08023	.00477	.00855	.00099
.09257	.00998	.01377	.00619
.10121	.01229	.01572	.00886
.10615	.01305	.01609	.01001
.11109	.01333	.01581	e01085
.11355	.01326	.01538	.01114
.11602	.01294	.01464	.01124
.11726	.01266	.01412	.01120
.11849	.01234	.01354	.01114
.11973	.01198	.01291	.01105
.12096	.01143	.01207	.01079
.12219	.01076	.01109	.01043
.12343	.00960	.00960	.00960
$\frac{x}{l}$ = 0.75			
0.05038	-0.01930	-0.01930	-0.01930
.05290	-.01750	-.01725	-.01775
.06348	-.00912	-.00790	-.01034
.07406	-.00176	.00030	-.00382
.08596	.00481	.00759	.00203
.09918	.01043	.01362	.00724
.10844	.01295	.01608	.00982
.11373	.01380	.01666	.01094
.11902	.01413	.01655	.01171
.12167	.01408	.01618	.01198
.12431	.01374	.01546	.01202
.12563	.01345	.01495	.01195
.12696	.01312	.01436	.01188
.12828	.01274	.01371	.01177
.12960	.01216	.01284	.01148
.13092	.01145	.01180	.01110
.13225	.01021	.01021	.01021

TABLE 11.- ORDINATES FOR 80° *SWEPT* ARROW WING WITH CAMBER AND TWIST - Concluded

$\frac{y}{l}$	$\frac{z_c}{l}$	$\frac{z_u}{l}$	$\frac{z_l}{l}$
$\frac{x}{l}$ = 0.80			
0.07557	-0.00435	-0.00435	-0.00435
.07899	-.00216	-.00184	.00248
.09169	.00481	.00624	.00338
.10580	.01084	.01315	.00853
.11567	.01358	.01614	.01102
.12131	.01452	.01703	.01202
.12696	.01490	.01714	.01266
.12978	.01487	.01688	.01286
.13260	.01453	.01622	.01284
.13401	.01423	.01572	.01274
.13542	.01388	.01514	.01262
.13683	.01348	.01446	.01250
.13824	.01288	.01358	.01218
.13965	.01212	.01249	.01175
.14106	.01087	.01087	.01087
$\frac{x}{l}$ = 0.85			
0.10076	0.00635	0.00635	0.00635
.11241	.01122	.01226	.01018
.12290	.01417	.01588	.01246
.12890	.01521	.01711	.01331
.13489	.01566	.01755	.01377
.13789	.01565	.01742	.01388
.14089	.01530	.01685	.01375
.14238	.01499	.01639	.01359
.14388	.01463	.01585	.01341
.14538	.01421	.01520	.01322
.14688	.01358	.01429	.01287
.14838	.01279	.01317	.01241
.14988	.01140	.01140	.01140

$\frac{y}{l}$	$\frac{z_c}{l}$	$\frac{z_u}{l}$	$\frac{z_l}{l}$
$\frac{x}{l}$ = 0.90			
0.12595	0.01355	0.01355	0.01355
.13013	.01474	.01514	.01434
.13648	.01588	.01678	.01498
.14282	.01640	.01762	.01518
.14600	.01640	.01768	.01512
.14917	.01606	.01730	.01482
.15076	.01574	.01692	.01456
.15235	.01537	.01644	.01430
.15393	.01493	.01587	.01399
.15552	.01428	.01497	.01359
.15711	.01344	.01383	.01305
.15869	.01198	.01198	.01198
$\frac{x}{l}$ = 0.95			
0.15114	0.01700	0.01700	0.01700
.15411	.01715	.01742	.01688
.15746	.01680	.01731	.01629
.15914	.01647	.01707	.01587
.16081	.01609	.01673	.01545
.16249	.01564	.01627	.01501
.16416	.01496	.01551	.01441
.16584	.01409	.01445	.01373
.16751	.01255	.01255	.01255
$\frac{x}{1}$ = 1.00			
0.17633	0.01311	0.01311	0.01311

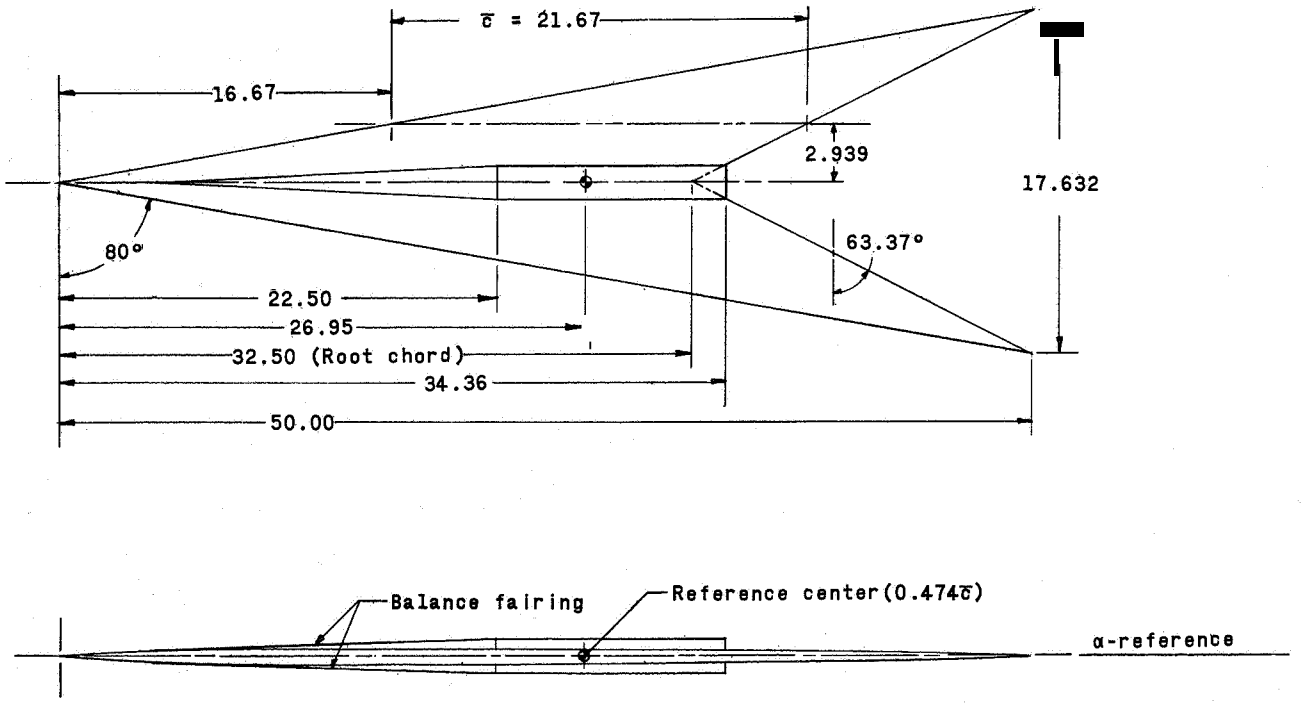

(a) Flat wing.

Figure 1.- Model drawings of 80° arrow wings. All dimensions are in inches unless otherwise noted.

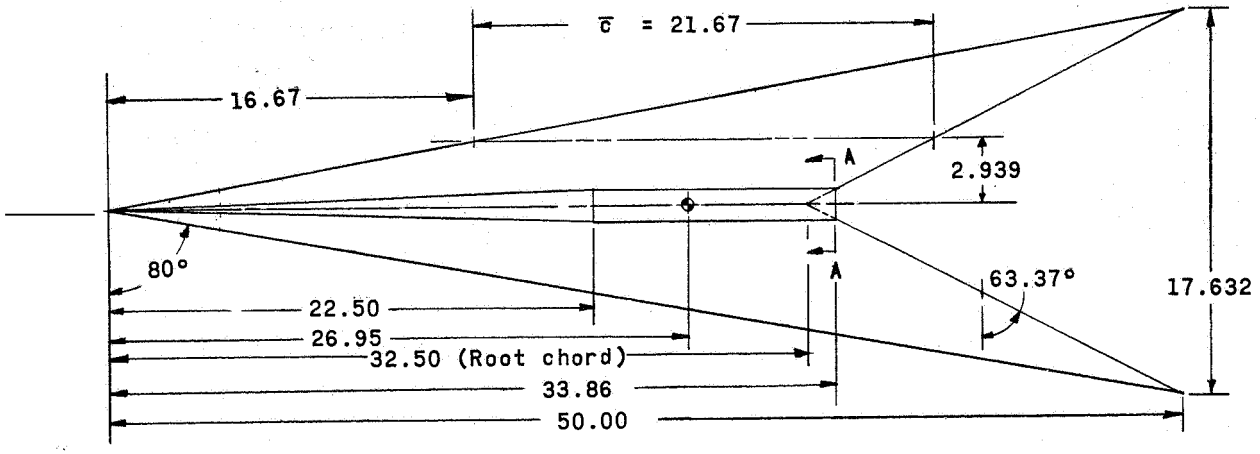

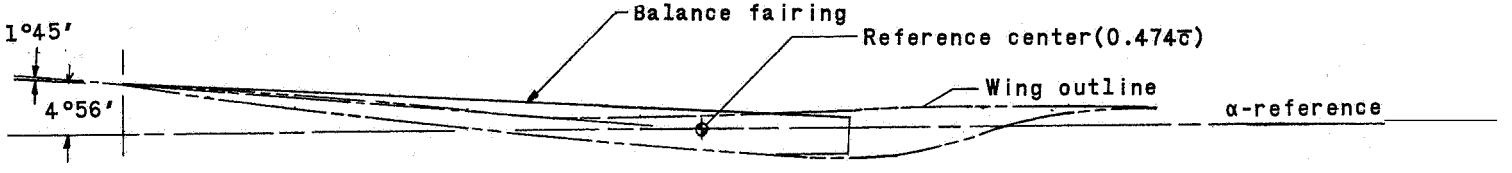

(b) Cambered and twisted wing.

Figure 1 - Concluded.

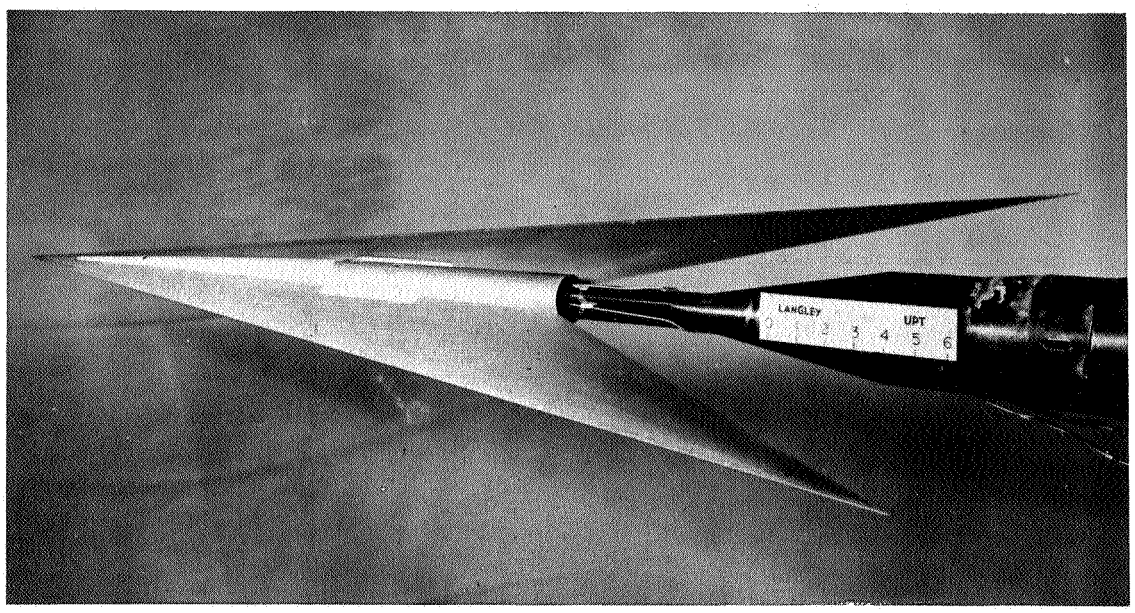

L-59-78

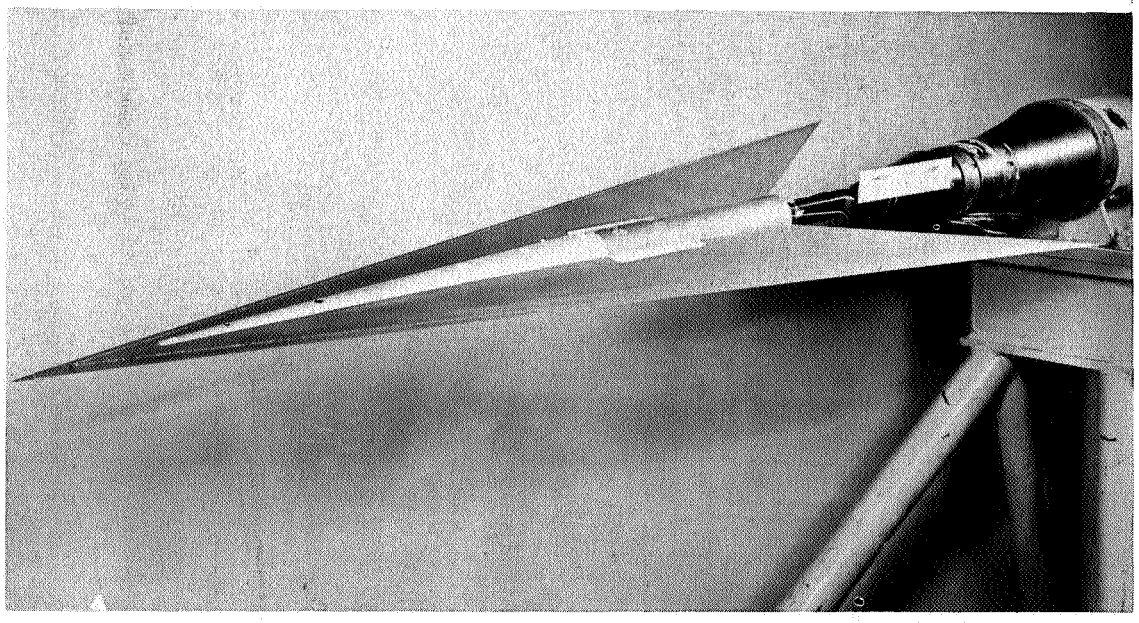

(a) Flat wing. L-59-80

Figure 2.- Models of the 80° swept arrow wings.

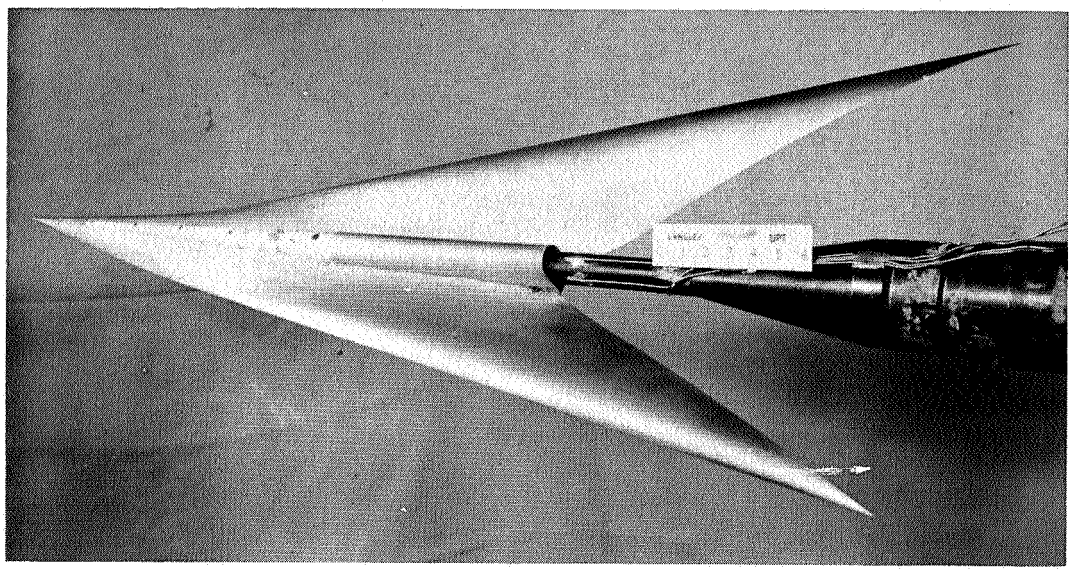

L-59-76

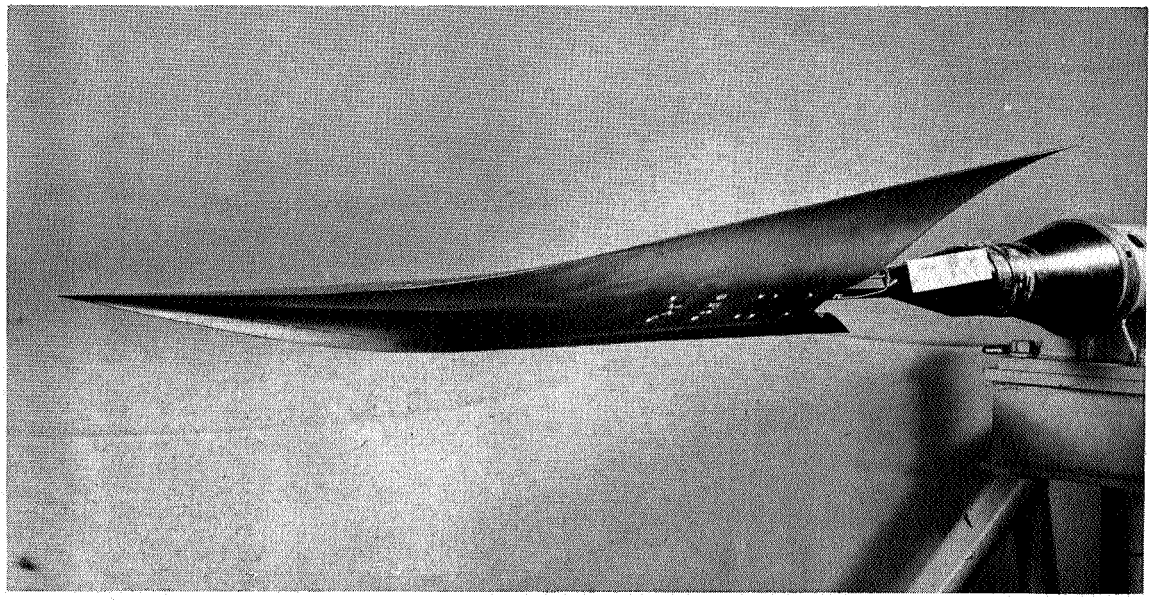

(b) **Cambered and twisted wing.** L-59-77

Figure 2.- Concluded.

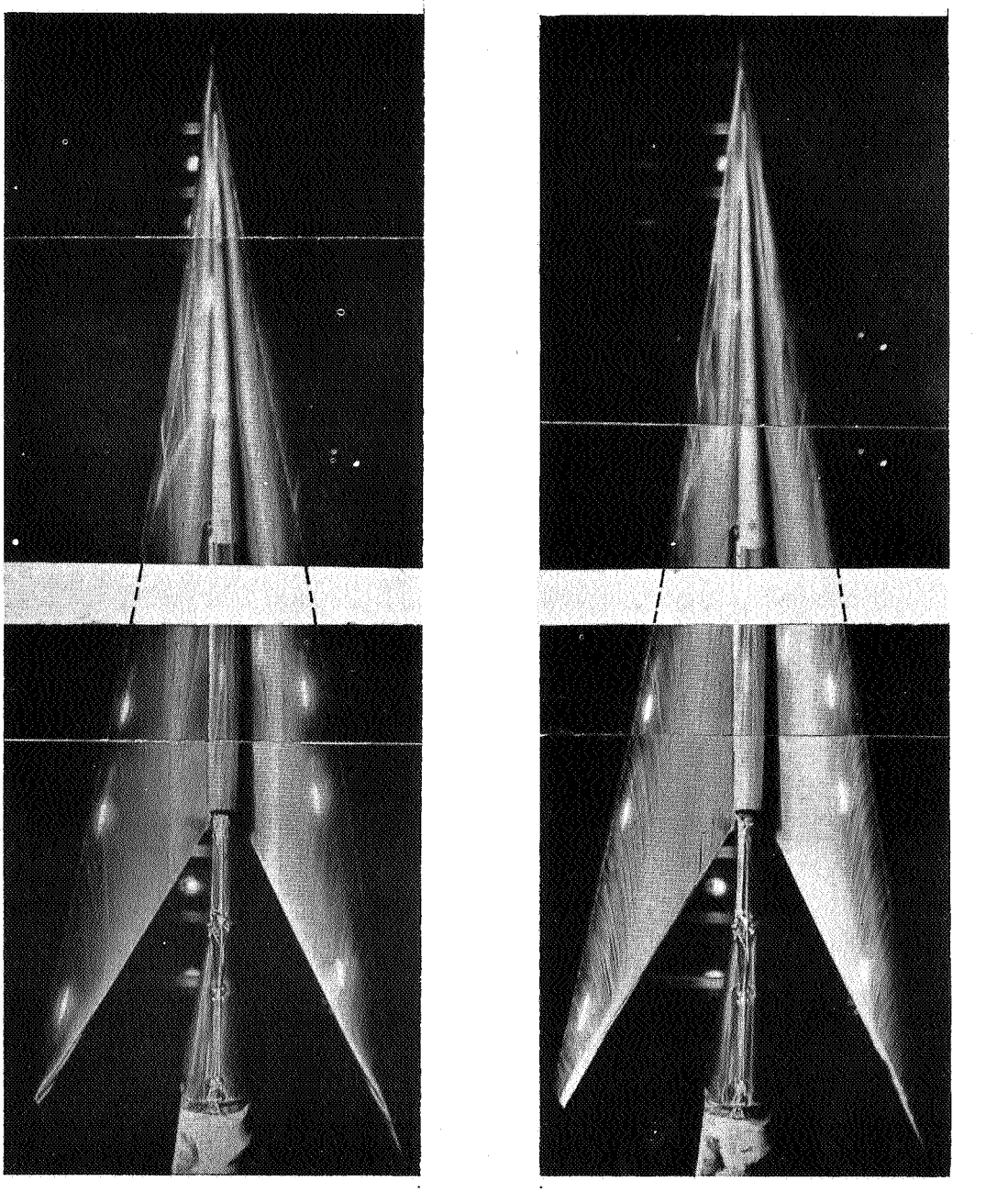

L-59-5047

(a) M = 2.29; C_L = 0.065. (b) M = 2.98; C_L = 0.036.

Figure 3.- Flow studies on 80° swept cambered and twisted arrow wing in which oil-film technique was utilized. Transition fixed; R = 5.0 x 10^6.

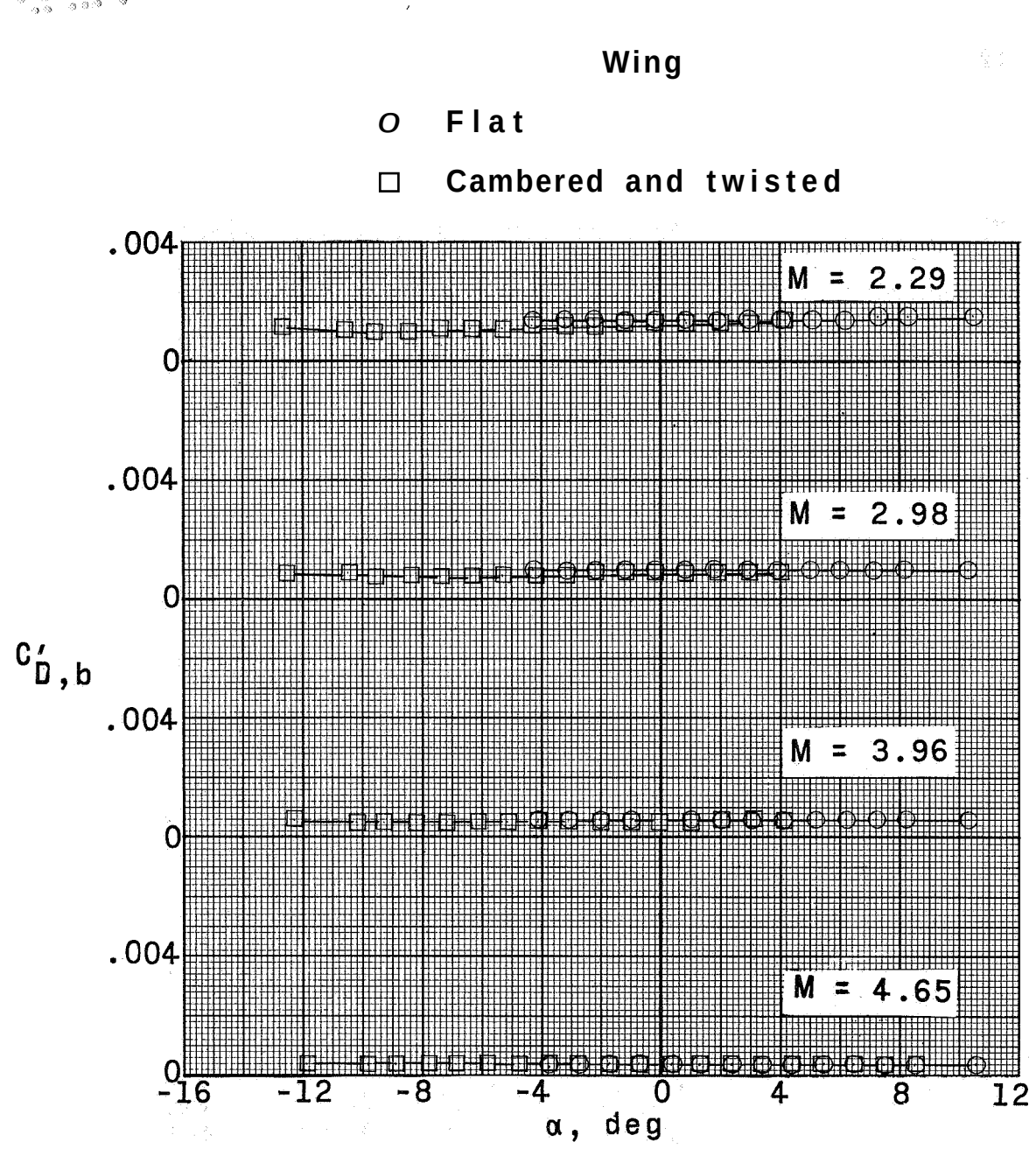

Figure 4.- Variation of base drag coefficient with angle of attack for the 80° swept arrow wings at $R = 5.0 \times 10^6$.

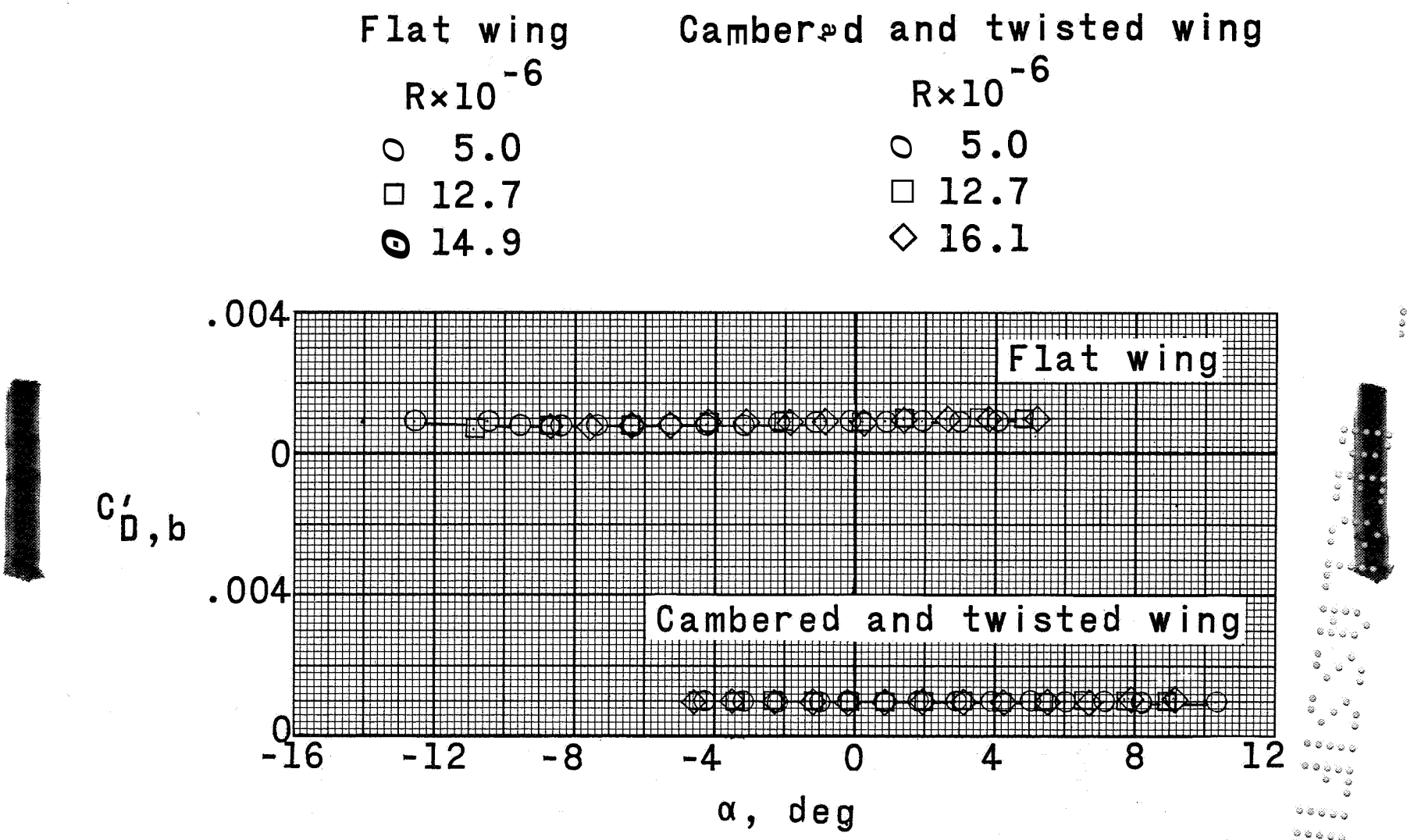

Figure 5 - Variation of base drag coefficient with angle of attack for several Reynolds numbers for 80° swept arrow wings at M = 2.98.

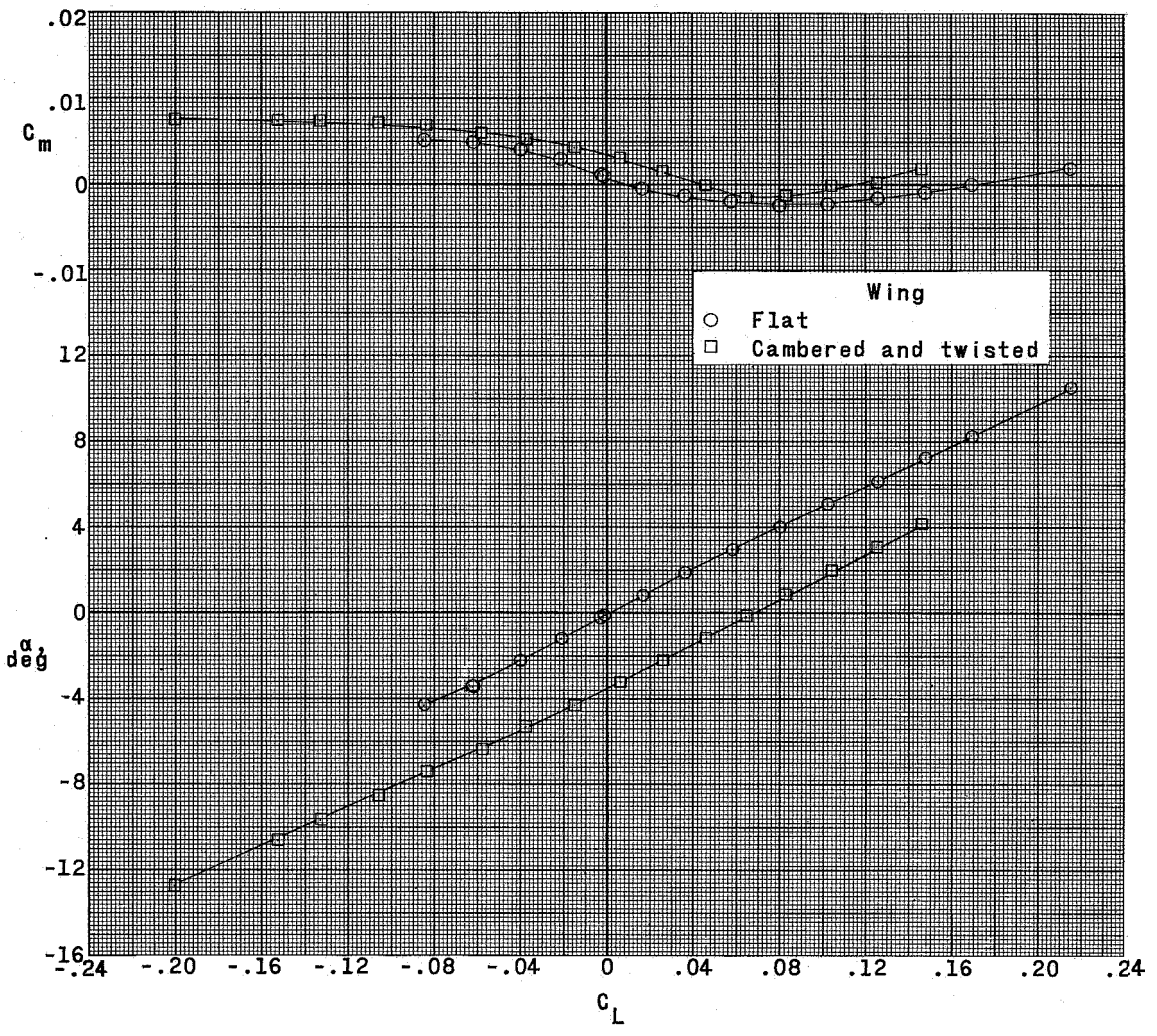

(a) M = 2.29.

Figure 6.- Longitudinal aerodynamic characteristics of 80° swept arrow wings at R = 5.0 x 10⁶.

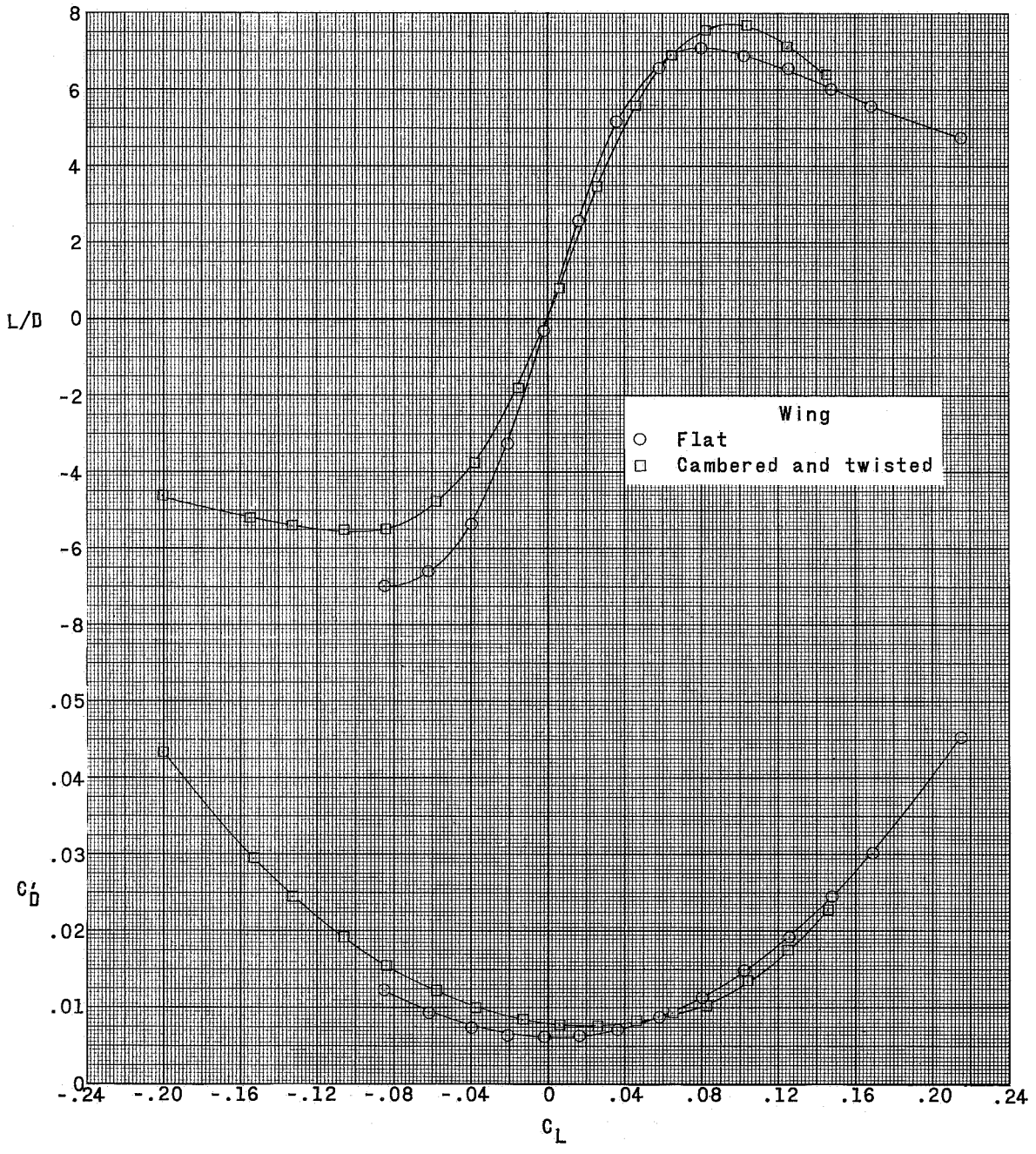

(a) Concluded.

Figure 6.- Continued.

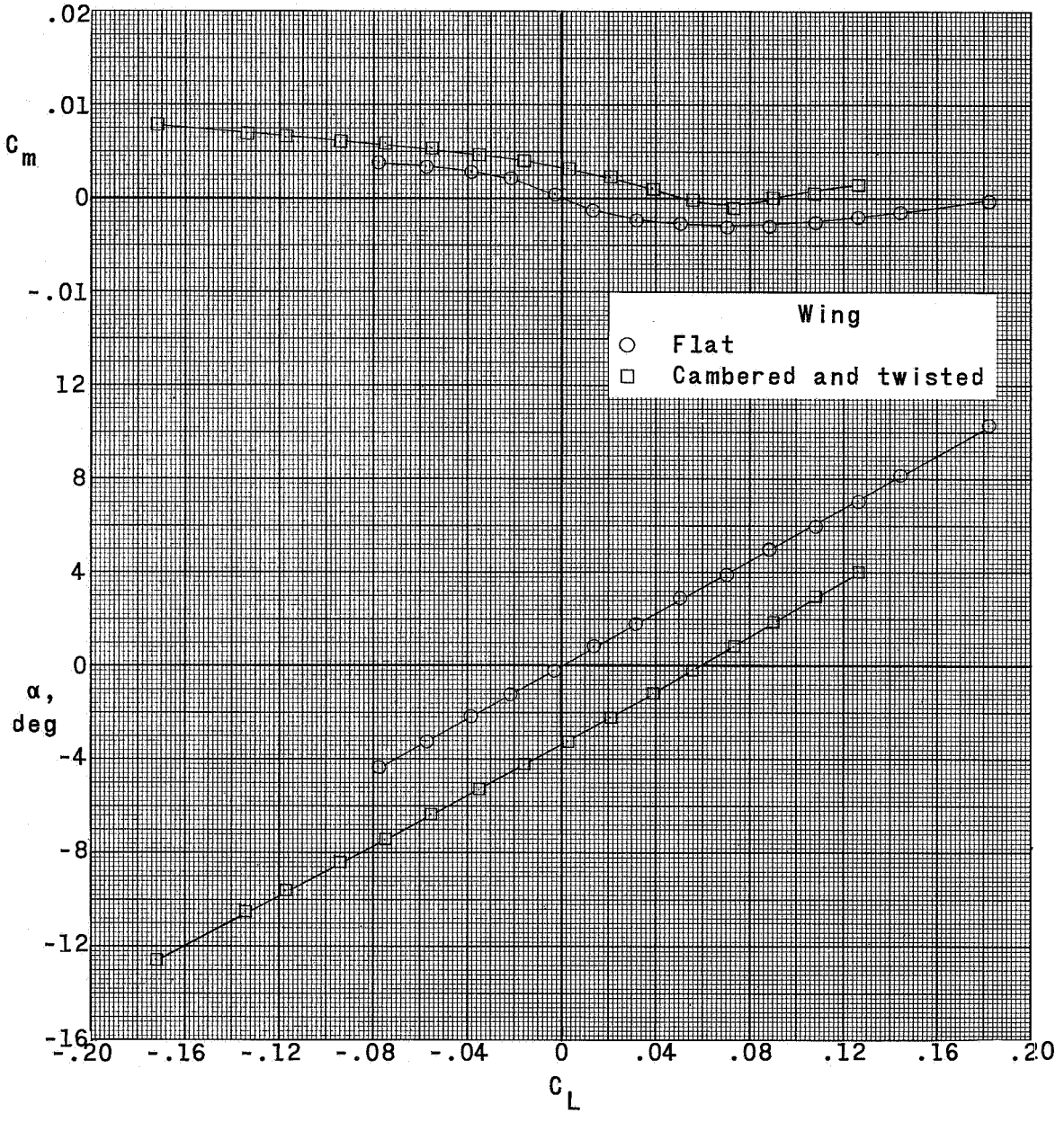

L-560

(b) M = *2.98.*

Figure 6.- Continued.

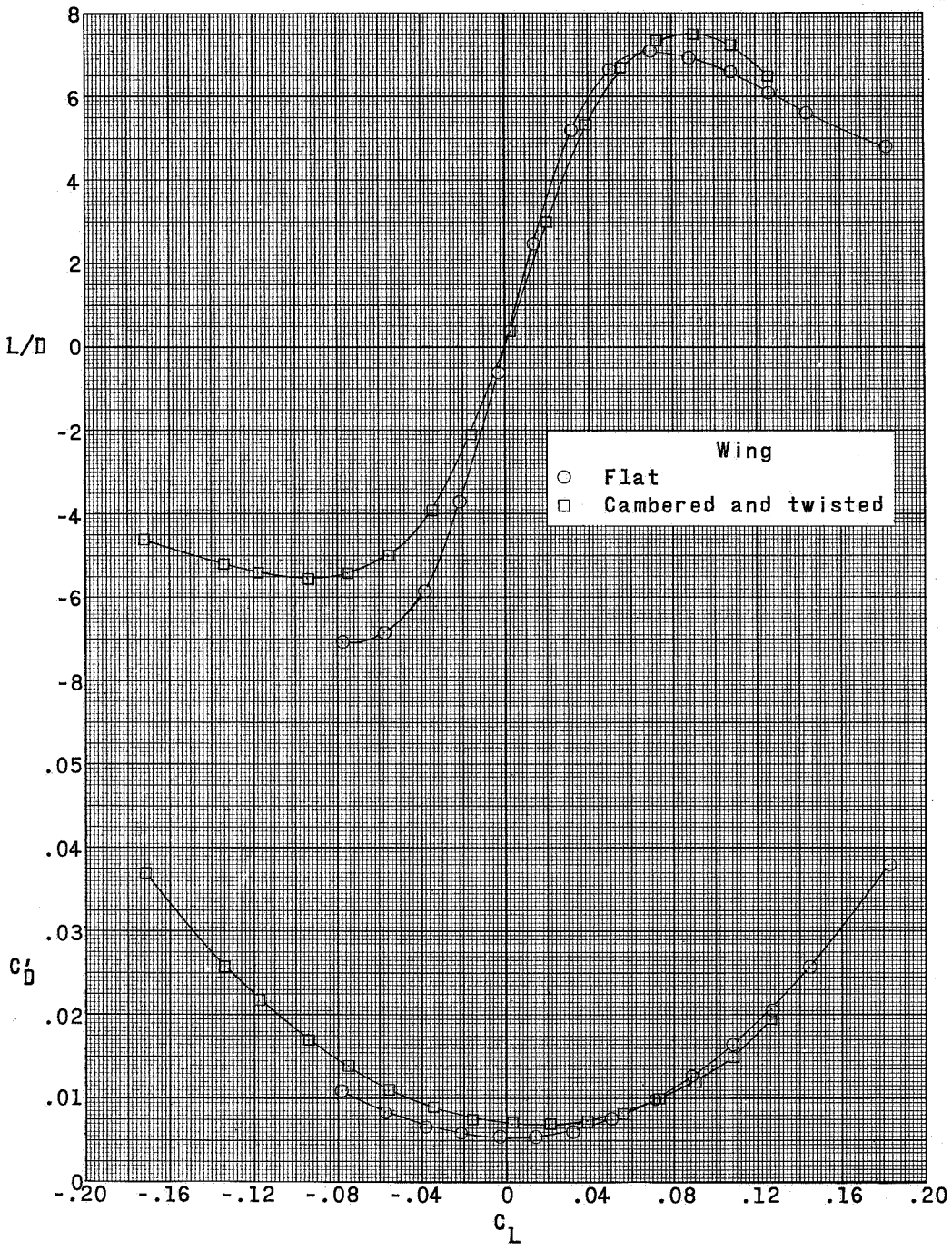

(b) Concluded.

Figure 6. - Continued.

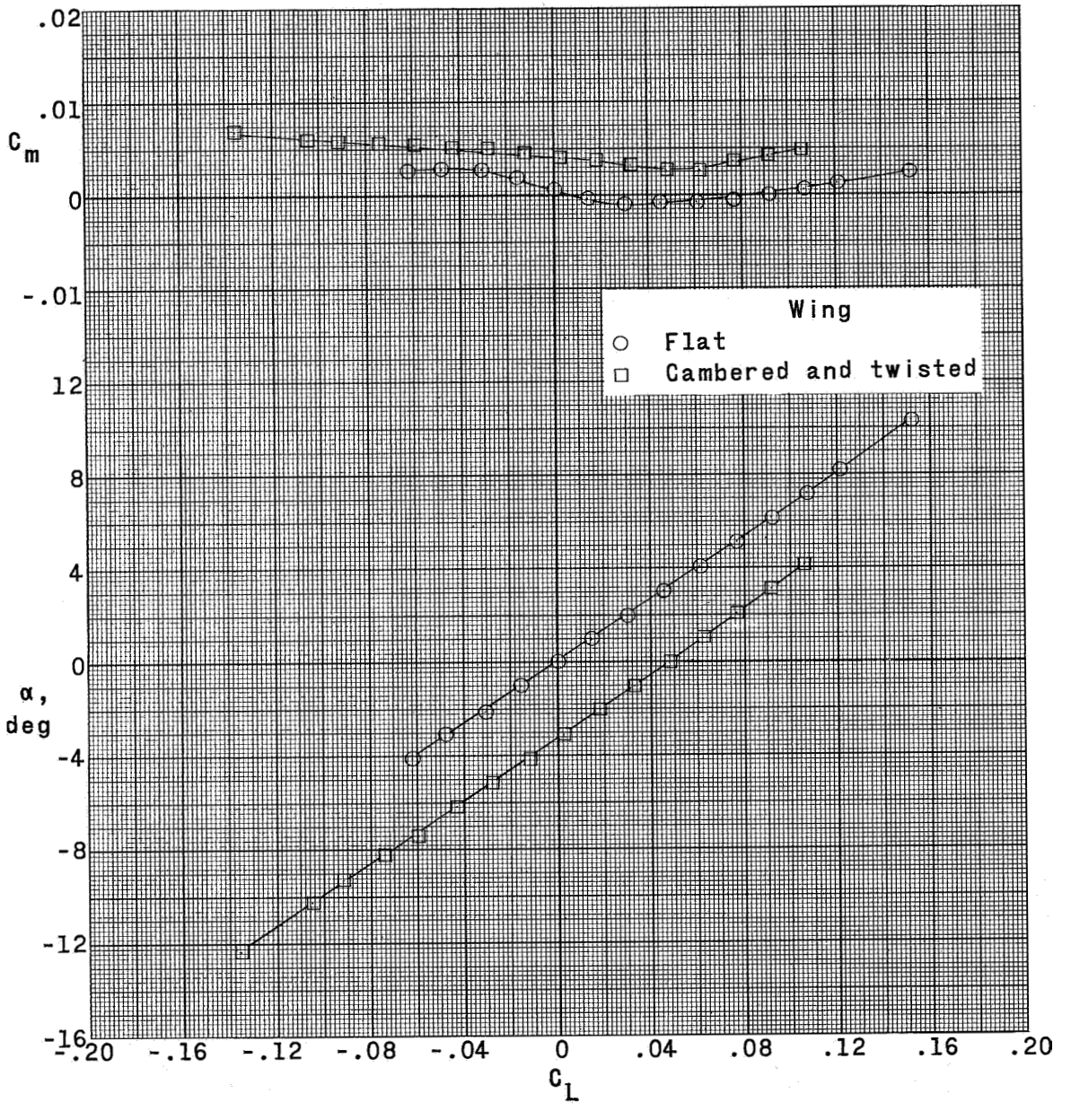

(c) M = 3.96.

Figure 6.- Continued.

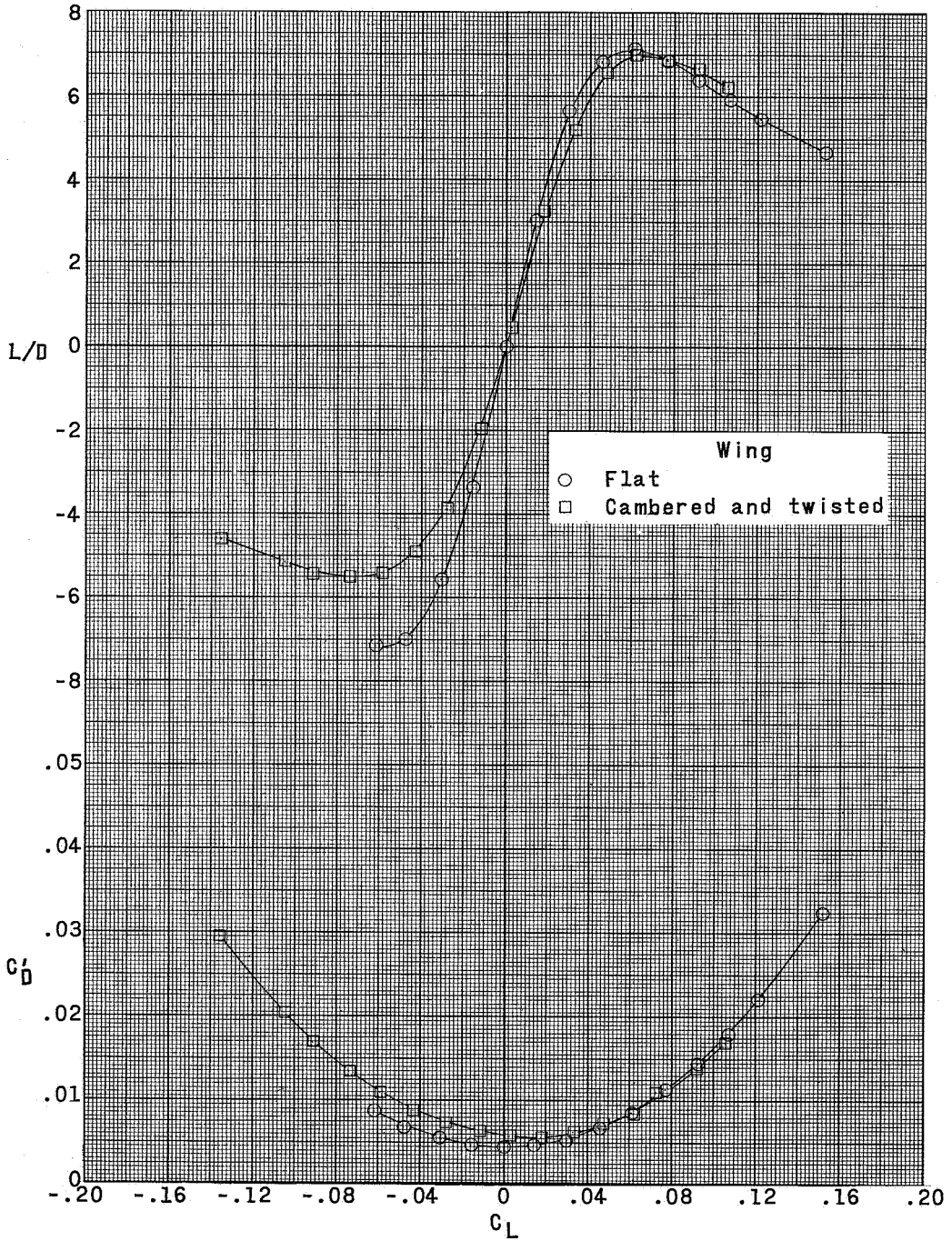

(c) Concluded.

Figure 6.- Continued.

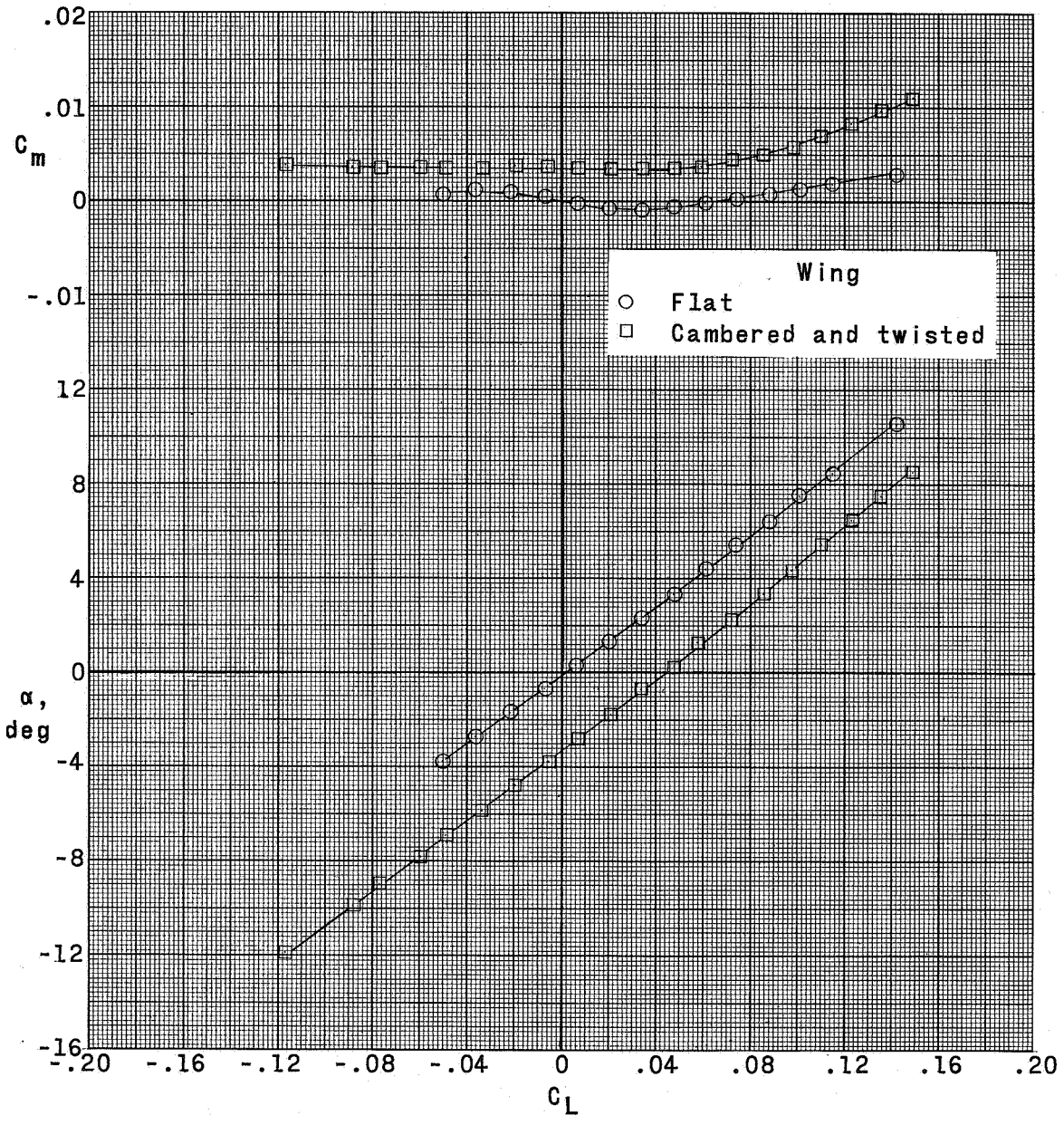

(d) M = 4.65.

Figure 6.- Continued.

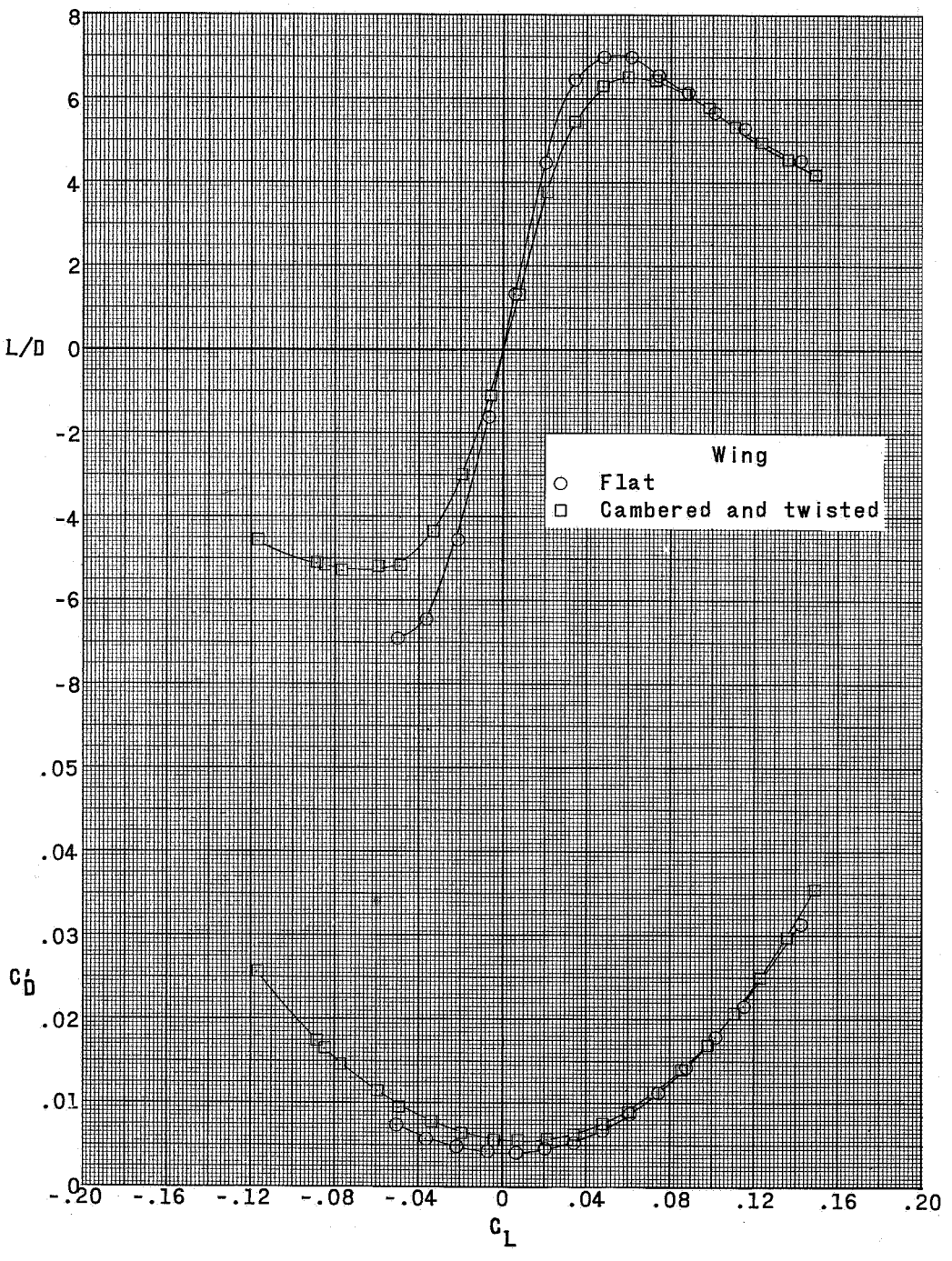

(d) Concluded.

Figure 6.- Concluded.

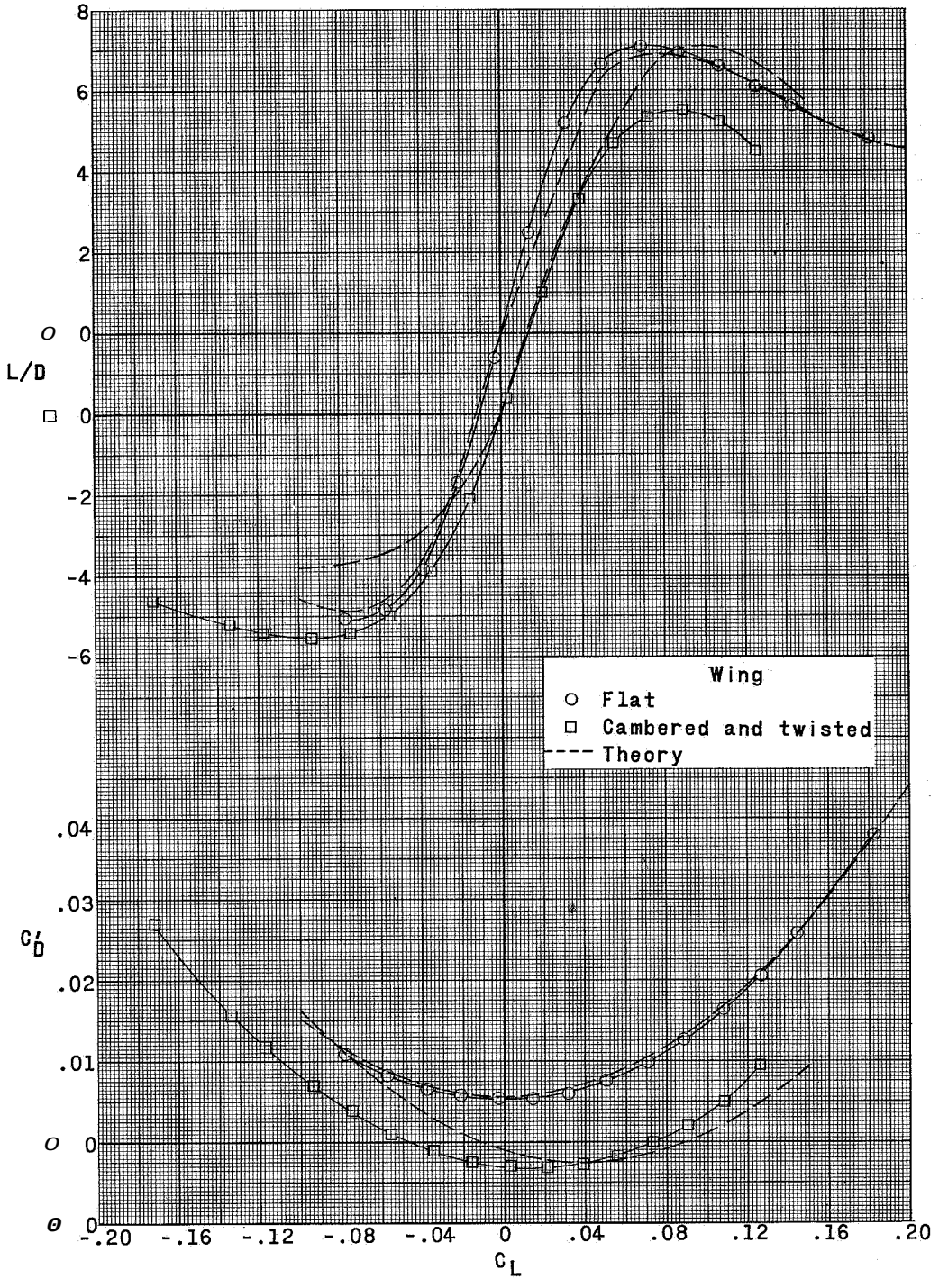

Figure 7.- Comparison of theoretical and experimental longitudinal aerodynamic characteristics at M = 2.98 and R = 5.0 x 10^6.

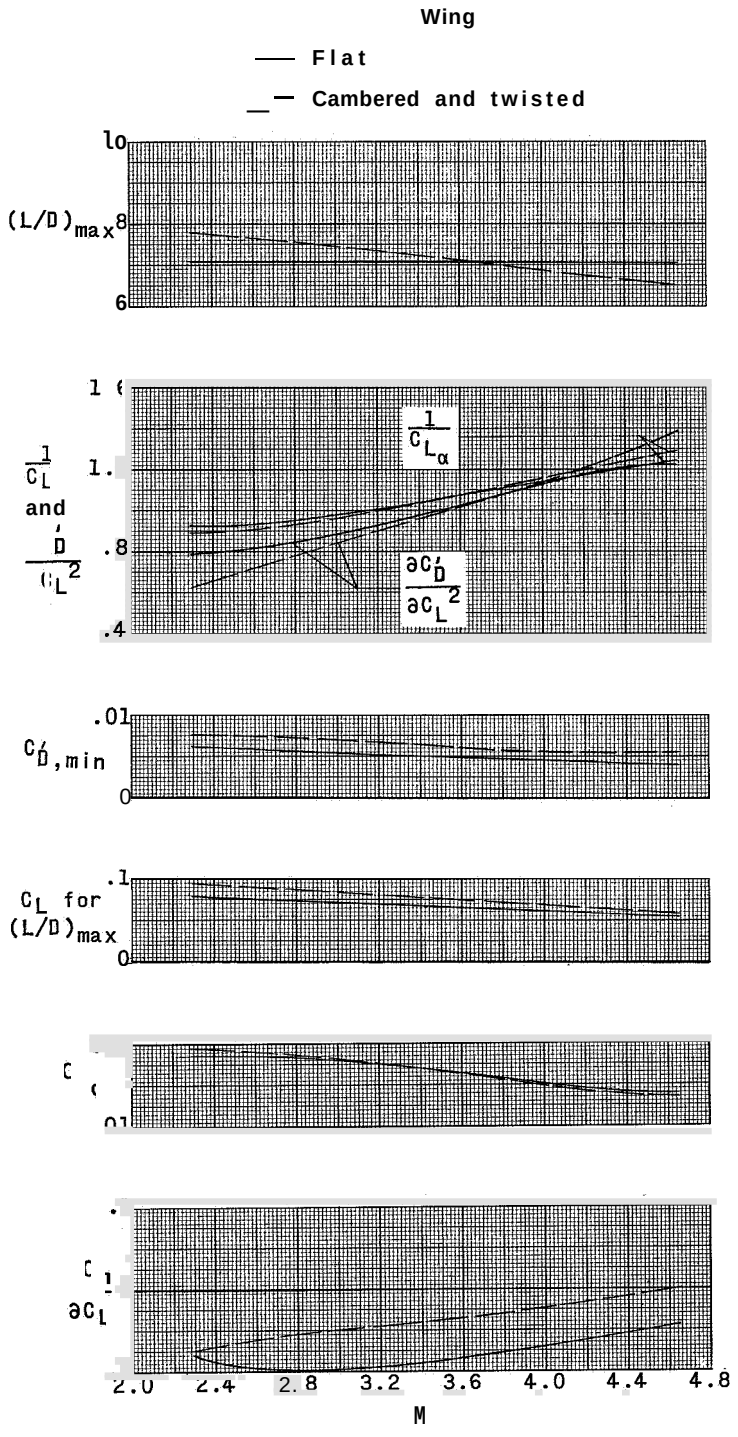

Figure 8.- Summary of the longitudinal aerodynamic characteristics for the 80° swept arrow wings.

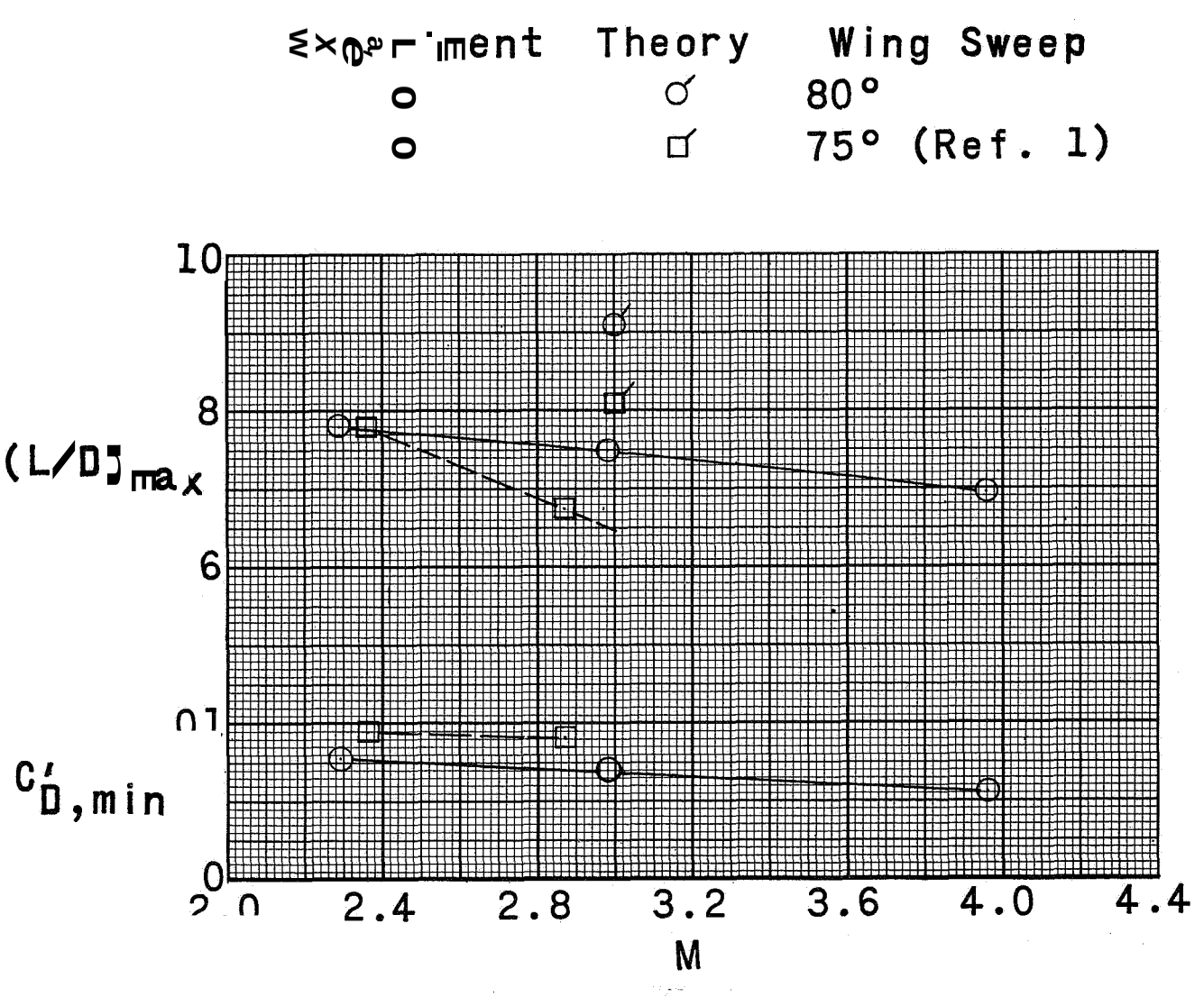

Figure 9.- Comparison of the variation of $C'_{D,min}$ and $(L/D)_{max}$ with Mach number of cambered and twisted arrow wings. Fixed transition.

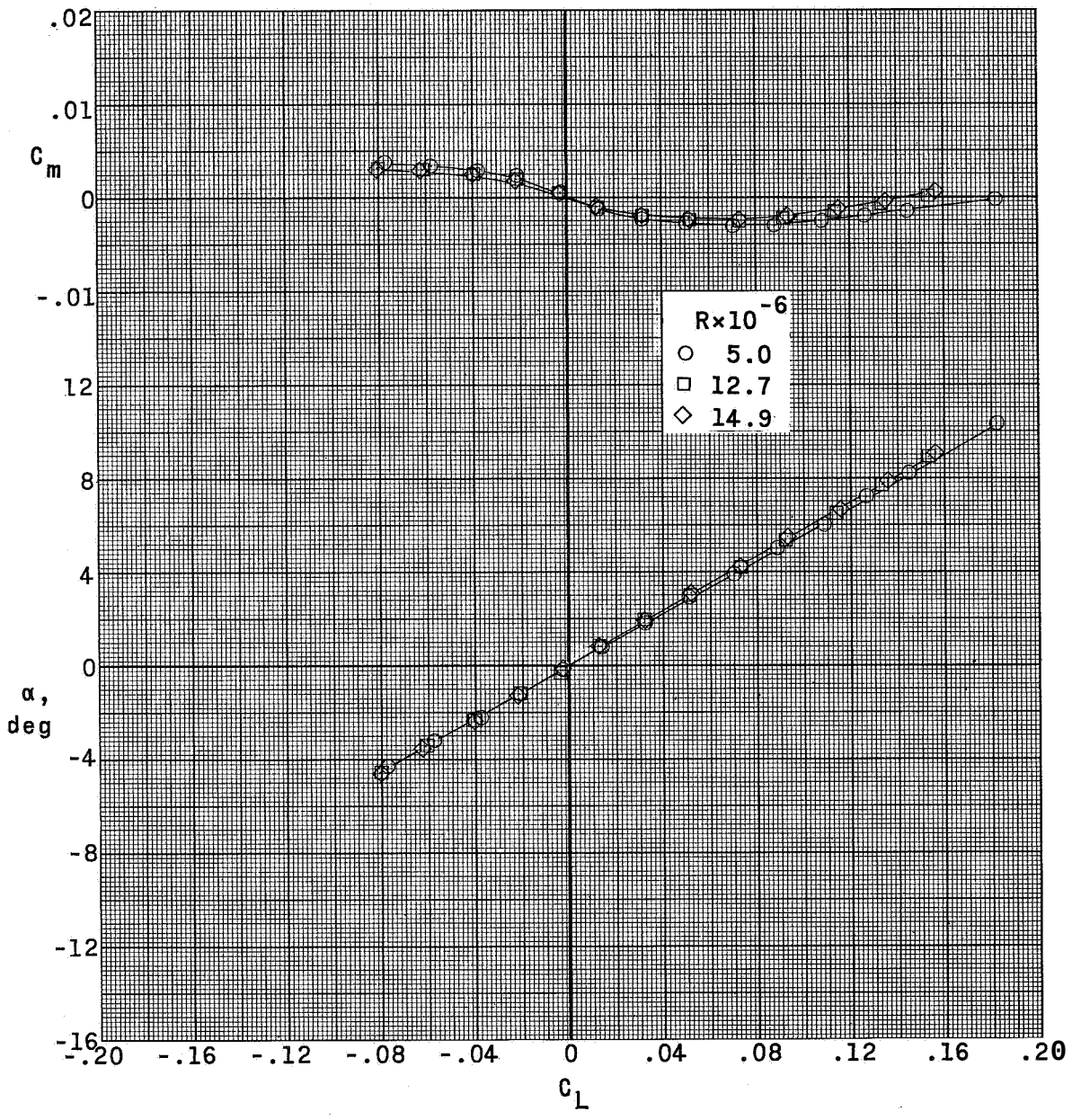

(a) Flat wing.

Figure 10.- Longitudinal aerodynamic characteristics at several Reynolds numbers for the 80° swept arrow wings at $M = 2.98$.

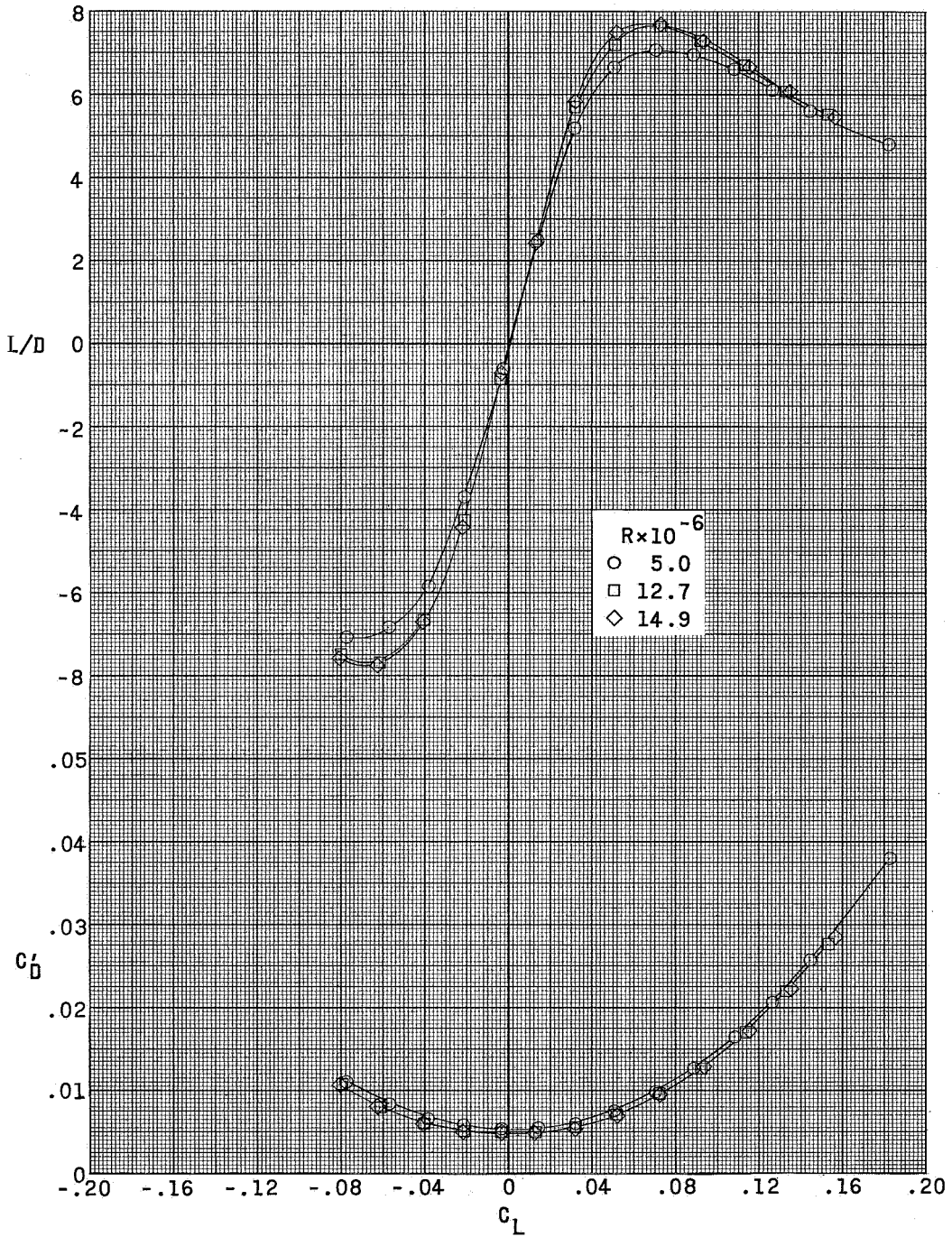

(a) Concluded.

Figure 10.- **Continued.**

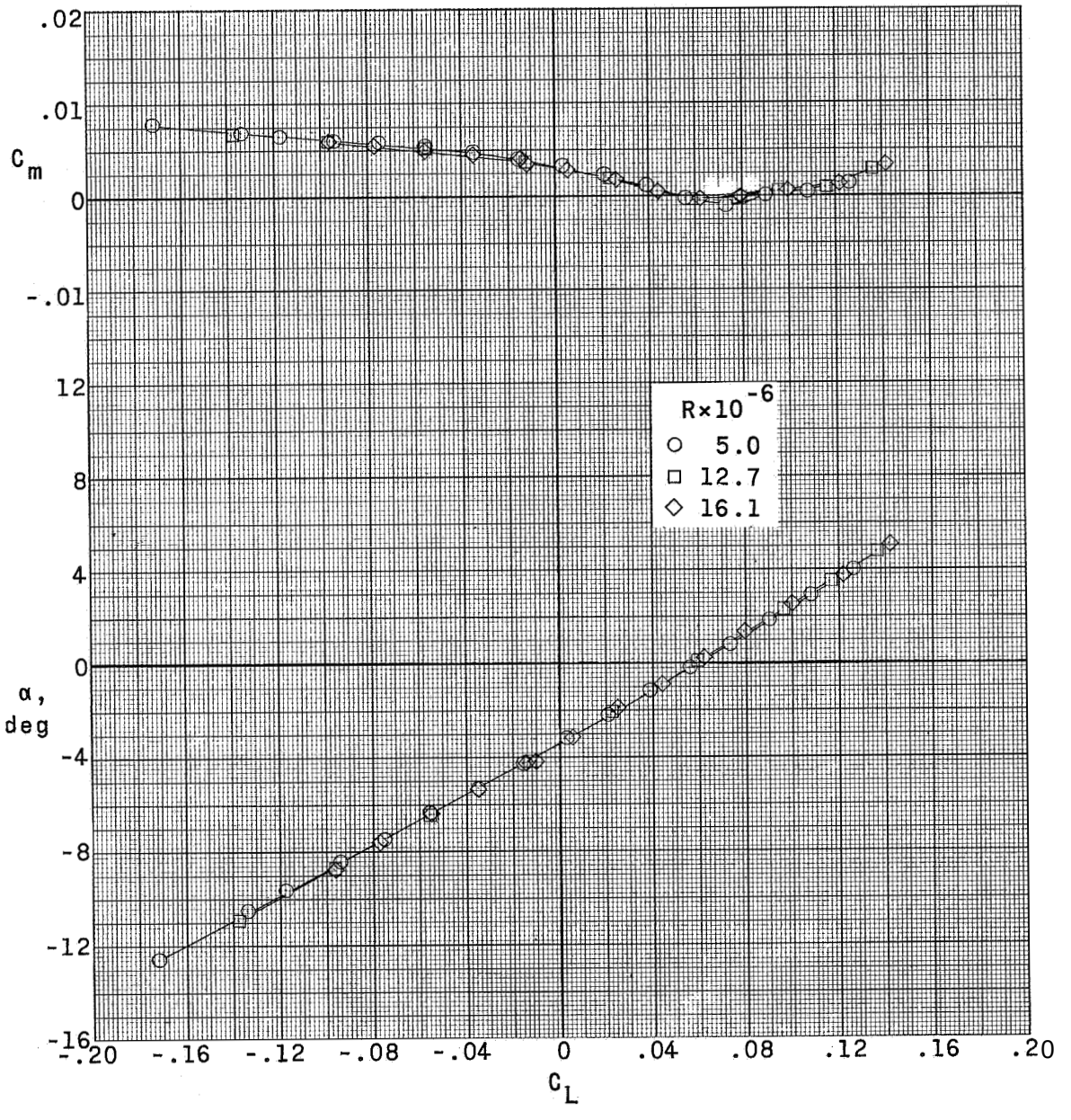

(b) Cambered and twisted wing.

Figure **10.-** Continued.

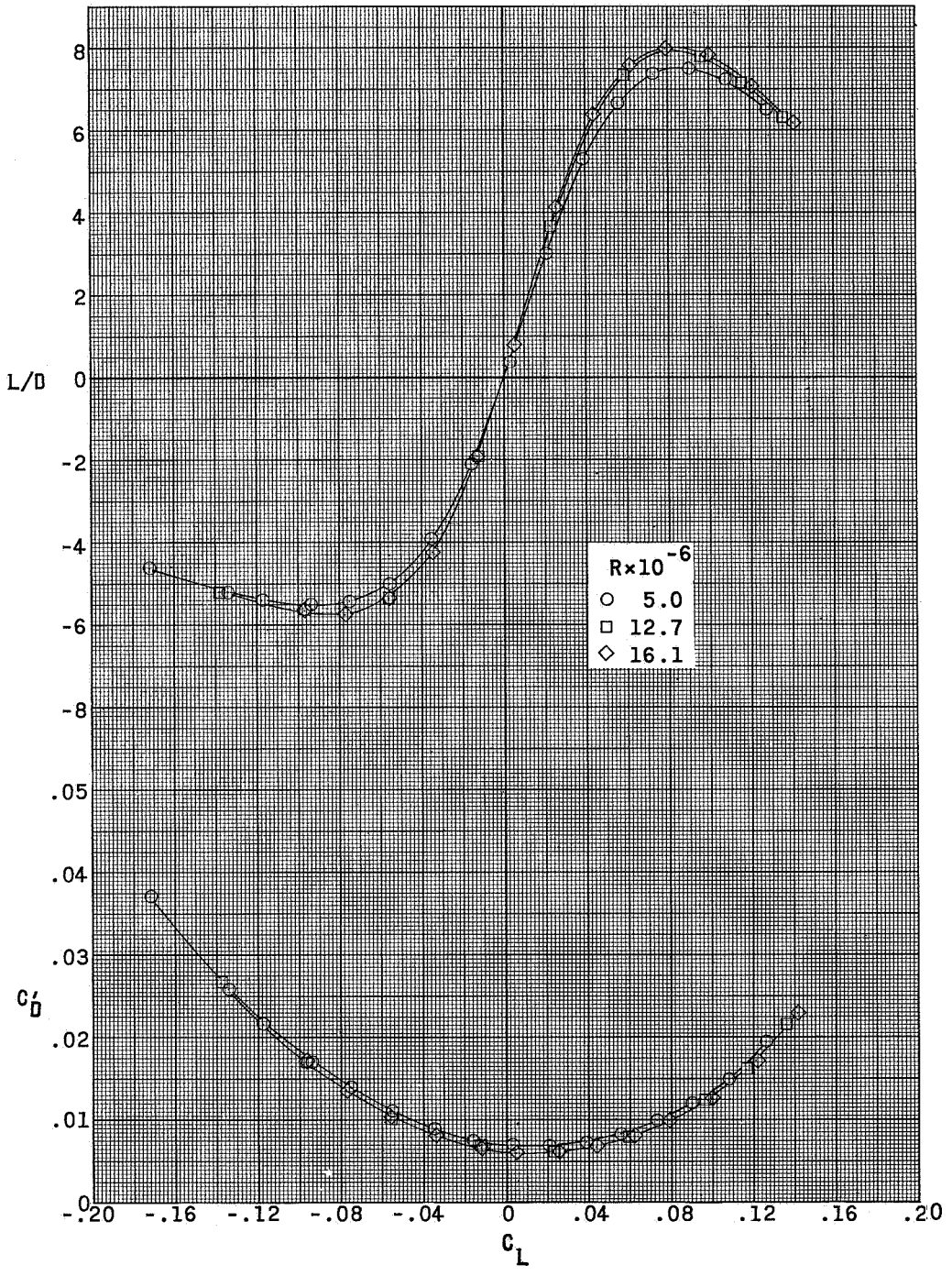

(b) Concluded.

Figure 10.- Concluded.

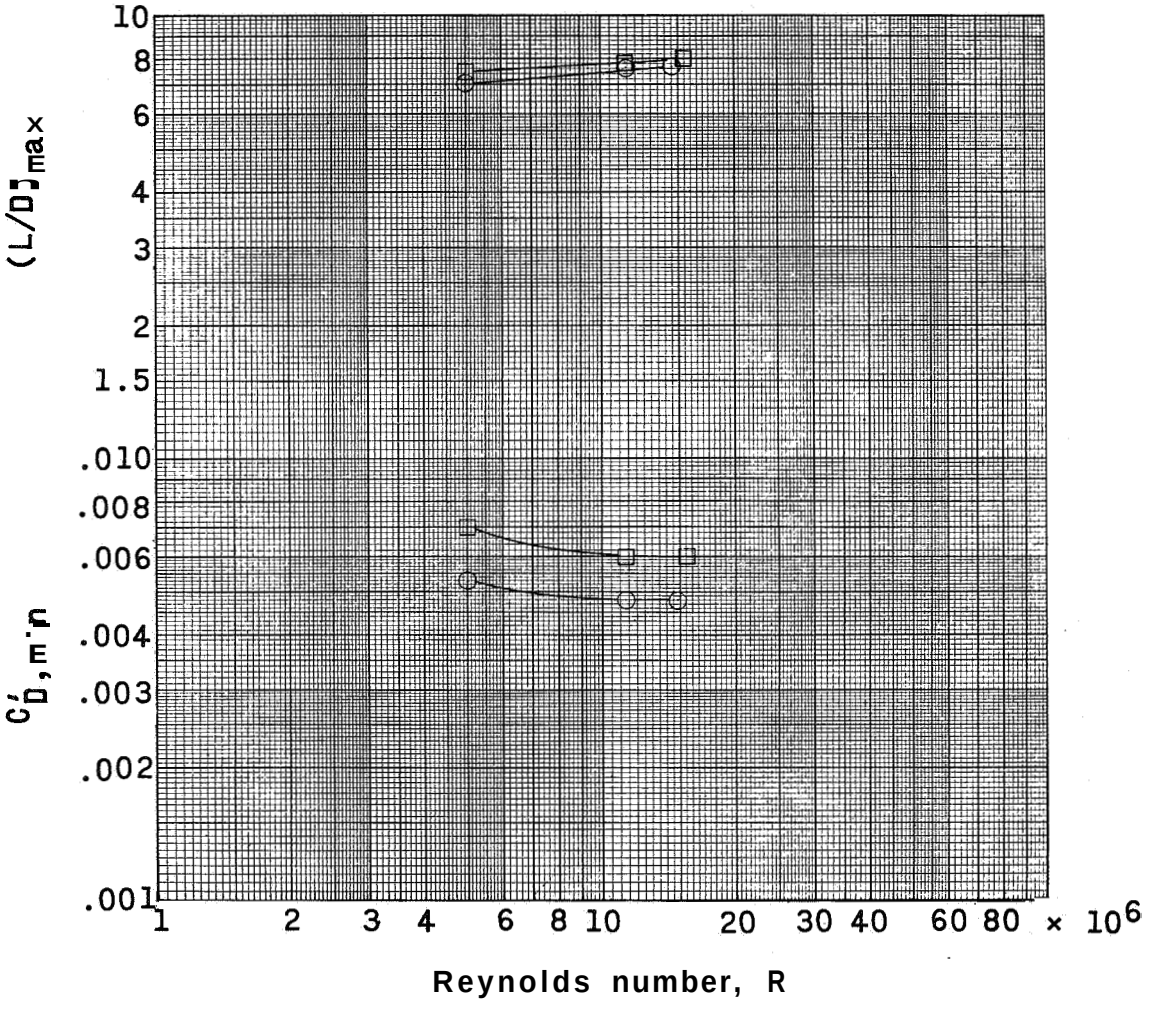

Figure 11.- Variation of $(L/D)_{max}$ and $C'_{D,min}$ with Reynolds numbers for the 80° swept arrow wings at M = 2.98.